ISSN 1075-7015, Geology of Ore Deposits, 2020, Vol. 62, No. 2, pp. 97–121. © Pleiades Publishing, Ltd., 2020.
Russian Text © The Author(s), 2020, published in Geologiya Rudnykh Mestorozhdenii, 2020, Vol. 62, No. 2, pp. 107–133.

ON THE 90TH ANNIVERSARY OF IGEM RAS

Valunistoe Epithermal Au–Ag Deposit (East Chukotka, Russia): Geological Structure, Mineralogical–Geochemical Peculiarities and Mineralization Conditions

A. V. Volkov[a], *, V. Yu. Prokof'ev[a], S. F. Vinokurov[a], O. V. Andreeva[a], G. D. Kiseleva[a], A. L. Galyamov[a], K. Yu. Murashov[a], and N. V. Sidorova[a]

[a] *Institute of Geology of Ore Deposits, Petrography, Mineralogy, and Geochemistry, Russian Academy of Sciences, Moscow, 119017 Russia*

**e-mail: alexandr@igem.ru*

Received January 21, 2019; revised November 18, 2019; accepted December 2, 2019

Abstract—The Valunistoe Au–Ag deposit is the third largest among epithermal deposits in Chukotka after the Kupol and Dvoinoe. It is located at the western closing of the East Chukotka flank zone of the Okhotsk-Chukotka volcanic belt. Volcanic domes (Pravogornenskaya, Zhil'ninskaya, Shakhskaya, Valunistaya, Shalaya, and Oranzhevaya, each is 3–6 km in diameter) have the main ore-controlling significance in the area; they form a chain elongated to the northeast, along the Kanchalan fault zone. Near the deposit, Upper Cretaceous volcanics are widespread: ignimbrites, lavas and tuffs ranging from rhyolite to basaltic composition, and lenses and interbeds of sedimentary rocks, subvolcanic bodies and dikes of andesites, basalts, and dacites. The structure of the deposit is caused by its localization within the limits of the eponymous (Valunistaya) volcanic dome. Twelve ore-bearing vein zones with thicknesses ranging from several to several tens of meters have been revealed at the deposit. The Glavnaya (Main) and Novaya (New) vein zones have been studied in detail; they are traced along their strikes to a distance of more than 1500 m and consist of en echelon veins 1.0 m thick on average, with lengths varying from 100 to 400 m. Based on the sampling data, Au and Ag contents in ores are 0–474.3 and 0–3794.23 g/t, respectively. Colloform-banded structures are frequently encountered, often combined with breccia structures. The main vein minerals are quartz and adularia; calcite, chlorite, fluorite, sericite, pyrophyllite, kaolinite, montmorillonite, gypsum, and epidote are less frequent. The main ore minerals are pyrite, acanthite, chalcopyrite, galena, sphalerite; secondary ore minerals are native Au and Ag and polybasite; rare ore minerals are pearceite, magnetite, hematite, marcasite, freibergite, tetrahedrite, bournonite, hessite, matildite, and others. Ores are characterized by an Au/Ag ratio from 1 : 5 to 1 : 10 and sulfidity (0.5–5%). Ores are enriched in many elements (Au, Ag, Sb, Cd, Pb, Cu, Zn, As, Se, Mo, Te, and Cr), with enrichment factors ranging from several times (Se, Mo, Te, and Cr), to tenfold (Cd, Pb, Cu, and Zn) and hundredfold (Sb) levels, reaching an excess of tens and hundreds thousand times for Au and Ag (Fig. 7). Ores are characterized by a low total REE and demonstrate positive Eu anomalies. Geochemical features are consistent with the mineral composition of ores. Full homogenization of fluid inclusions in quartz occurs at temperatures of 203–284°C and 174–237°C in calcite, while the salt concentration in both cases is from 0.2 to 0.7 wt % NaCl equiv. Fluid density changes from 0.87 to 0.56 g/cm^3. The results give grounds to attribute the Valunistoe deposit to the low-sulfidized epithermal class. The data provided in the article are of practical value for regional forecast–metallogenic maps and can be used in searching for and appraising epithermal Au–Ag deposits.

Keywords: East Chukotka, deposit, epithermal, ore mineralization, gold, silver, trace elements, fluid inclusions, mineralization conditions

DOI: 10.1134/S1075701520020075

INTRODUCTION

The Valunistoe deposit is located in Russia's Arctic zone, in the territory of Anadyr district of the Chukotka Autonomous Okrug (ChAO), 237 km northeast of the regional center of Anadyr, at the 218th km marker on the automobile road from the nearest seaport of Egvekinot (Fig. 1).

This deposit was discovered in the 1960s by geologists of the Anadyr expedition. Geological surveys there were periodically conducted up until 1996 (Shabalin et al., 1995*, 2000*[1]). Based on the results of

[1] Hereinafter, "*" after the year of a reference denotes a production report stored in the holdings of Rosgeolfond (Russian Fund for Geology).

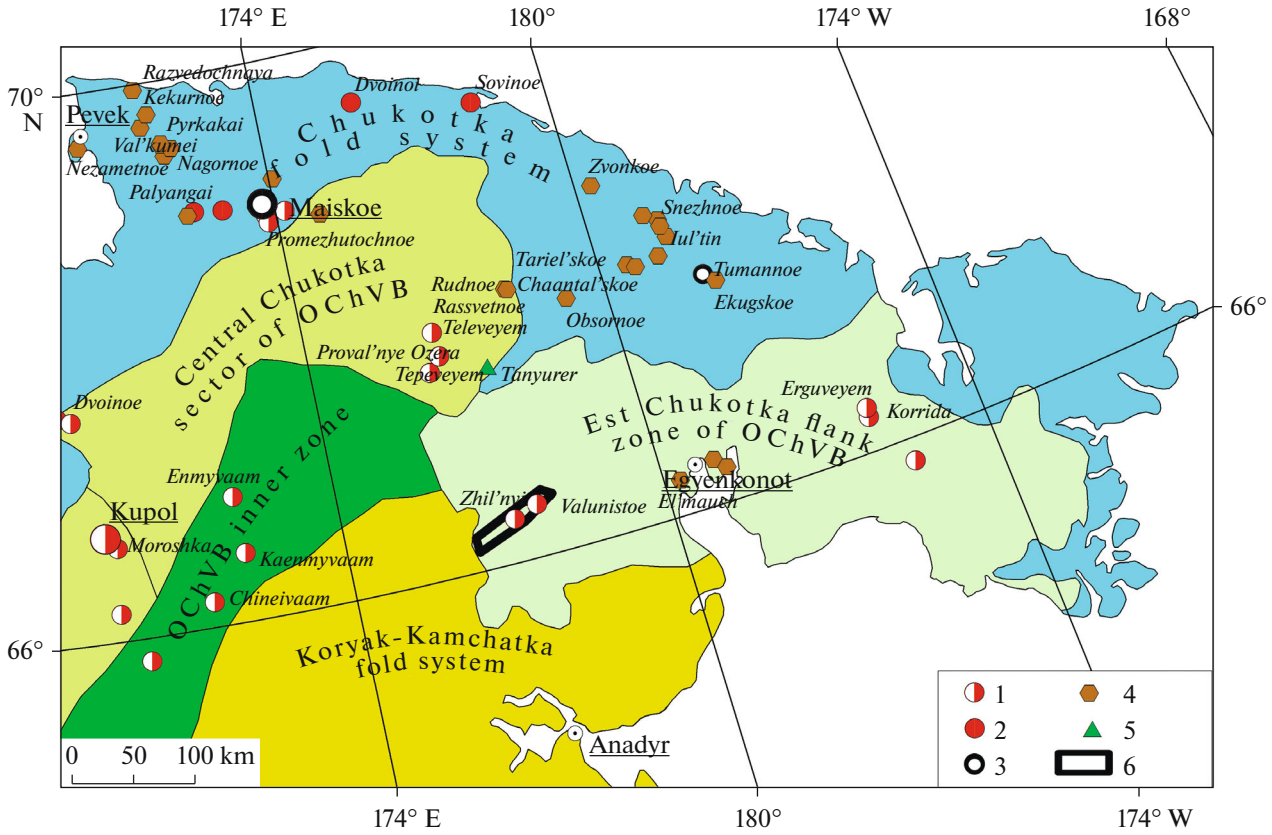

Fig. 1. Position of Valunistoe deposit in regional structures, based on scheme by V.F. Belyi (1994). (1–5) Deposits: ((1) Au–Ag epithermal, (2) Au–quartz, (3) impregnated Au-sulfide, (4) tin-ore; (5) copper-porphyry; (6) Amguema-Kanchalan metallogenic zone.

these works, the $C_1 + C_2$ balance reserves were 17.5 t Au with an average content of 5.9 g/t and 178 t of Ag with an average content of 59.6 g/t.

In 1999, the surveying and operating rights of the deposit were sold at auction to the Chukotka mining cooperative. In 2011, control over the Valunistoe deposit was gained by Aristus Holdings Limited (Cyprus), affiliated with Millhouse company. Finally, at the end of 2018, the deposit was bought by Highland Gold Mining Limited.

In total, since 1999 until 2017 inclusive, more than 18 t of Au and 157 t of Ag have been recovered at the three quarries of the deposits. In 2017, according to the ChAO administration, the amounts of Au and Ag extracted from ores of the Valunistoe deposit were 862.53 kg and 7.506 t, respectively. According to the data from Highland Gold Mining Limited (https://www.highlandgold.com), the reserve life for the Valunistyi mine is more than 10 years.

In the late 20th century, the geological structure of the Amguema-Kanchalan metallogenic zone, which includes the Valunistoe deposit, was considered in a number of research publications in terms of petrology, geochemistry, and geodynamics of volcanoplutonic associations (Polin, 1990); in particular, the regional forecast map (for the Okhotsk-Chukotka volcanic belt, or OChVB) on a scale of 1 : 500000 was compiled (Bocharnikov, 1980*); and the additional site appraisal report on GDP-200 was carried out (Romanov, 2002*); etc.

In 2000–2019, prospecting and survey works were carried out, aimed at searching for new orebodies and actively increasing the reserves immediately at the ore field and Valunistoe deposit; first, they were conducted by the Artika mining cooperative (Shabalin et al., 2006*), then by OOO Artel' staratelei Chukotka (Lyashkevich et al., 2008*; Polkvoi et al., 2011*), OOO Regional'naya gornorudnaya kompaniya (Filonov et al., 2014*), and finally by OOO GeoSolutions (Kozlova et al., 2018*).

From 2012 to 2019, Institute of Geology of Ore Deposits, Petrography, Mineralogy, and Geochemistry, Russian Academy of Sciences (IGEM RAS), repeatedly investigated the mineralogical–geochemical and thermobarogeochemical features of the Val-

unistoe deposit ores: first, under the contract with OOO Rudnik Valunistyi (JSC Valunistyi Quarry), then with grant no. 14-17-00170 of the Russian Science Foundation, and in 2018–2019 with grant no. 18-05-70001 of the Russian Foundation for Basic Research.

The main objective of our studies was to analyze and generalize the available data on the geology of the deposit and to reveal mineral–geochemical specialization of gold-ore quartz veins (this specialization can help to appraise the degree of vein productivity). We should also note that studies on the composition and parameters of ore-forming fluids aimed at revealing their nature has remained the key problem in the theory of endogenic mineralization for many decades (see (Bortnikov, 2006) and others). In the present article, the results of comprehensive studies of the deposit are summarized.

STUDY METHODS

There is quite a large collection of epithermal ores and metasomatic rocks from the Valunistoe deposit at IGEM RAS, namely, 35 specimens, of which the majority (25) are represented by core fragments of well VD-12-1301 (Novaya (New) ore zone), and the rest ones were collected from vein bodies in quarries nos. 1 and 2 (Glavnaya (Main) ore zone).

The chemical composition of minerals was examined with a JXA-8100 electron probe microanalyzer (manufactured by JEOL, Japan) at the Laboratory for Mineral Material Analysis of IGEM RAS (analyst I.G. Griboedova). Analyses were carried out at an accelerating voltage of 20 kV and at Faraday cylinder current of 20 Na. The probe diameter was 3–5 μm. The exposure time for the main elements was 10 s. JEOL standards were used.

For chlorite and kaolinite diagnostics, we applied X-ray phase analysis with a D/MAX-2200 diffractometer (Ridaku company, Japan) equipped with modern software for acquisition and processing of experimental data. Studies were conducted by the X-ray group, Laboratory of Crystallochemistry, IGEM RAS.

The concentrations of rock-forming and particular admixture elements in samples were studied by X-ray fluorescence analysis on an Axios mAX serial-operating vacuum spectrometer with wavelength dispersion (PANalytical company, the Netherlands, 2012; www.panalytical.com). When calibrating the spectrometer, we used industrial and state standards of rock compositions. Analysis was carried out by the 439-PC technique (developed by the Scientific Council on Analytical Methods, Fedorovsky All-Russia Research Institute of Mineral Resources), making it possible to obtain results in accordance with OST RF (Industrial Standard of the Russian Federation) 41-08-205-04 (analyst A.I. Yakushev).

Trace element measurements (ICP-MS) were taken on an X-Series II inductively coupled plasma mass spectrometer (analyst Ya.V. Bychkova). The detection limits of elements ranged from 0.1 ng/g for heavy and medium elements and up to 1 ng/g for light elements. The error of analysis was 1–3 rel %. Au and Ag contents in samples were determined by atomic absorption spectrometry with electrothermal atomization on a Spectr AA220Z spectrometer (analyst V.A. Sychkova).

Microthermometric studies of individual inclusions were conducted at the Laboraty of Geology of Ore Deposits, IGEM RAS, using measurement equipment created on the basis of a THMSG–600 temperature-controlled stage (Linkam, England), an Olympus BX51 microscope equipped with a set of long-focus lenses, a video camera, and a controlling computer. This equipment enables real-time measurements of the phase transition temperatures within inclusions in the temperature range from –196 to 600°C, to observe them at large magnification, and to obtain electron microimages.

Compositions of salts dominant in the aqueous solutions of fluid inclusions were estimated from the measured eutectic melting temperatures (Borisenko, 1977). The total concentration of salts in two-phase fluid inclusions was inferred from ice melting temperatures based on experimental data for the NaCl–H_2O system (Bodnar and Vityk, 1994). Estimates of the salt concentration and fluid density were obtained with FLINCOR software (Brown, 1989).

The bulk composition of fluid inclusions was studied at the Analytical Laboratory of the Central Research Institute of Geological Prospecting (analyst Yu.V. Vasyuta) using the set of methods, including gas chromatography (Agilent 6890 chromatograph) and ion chromatography (TsVET 3000 chromatograph), as well as inductively coupled plasma mass spectrometry (ELAN 6100, PerkinElmer SCIEX company, United States), by the technique described in (Kryazhev et al., 2006).

POSITION IN REGIONAL STRUCTURES

The Valunistoe deposit is located at the western closure of the East Chukotka flank zone of the OChVB (Belyi, 1994; Sidorov et al., 2009), which encompasses the Koryak–Kamchatka fold zone (Fig. 1). Here, volcanic rocks of the OChVB fill a NE-oriented trough 30–100 km wide, traced from the Tanyurer River in the west to the Amguema River in the east (Romanov et al., 2002*). The folded basement of the trough is represented by dislocated Paleozoic deposits.

The main ore-controlling objects in the study area are the Pravogornenskaya, Zhil`ninskaya, Shakhskaya, Valunistaya, Shalaya, and Oranzhevaya volcanic domes, 3–6 km in diameter, forming a chain extending to the northeast along the Kanchalan fault zone

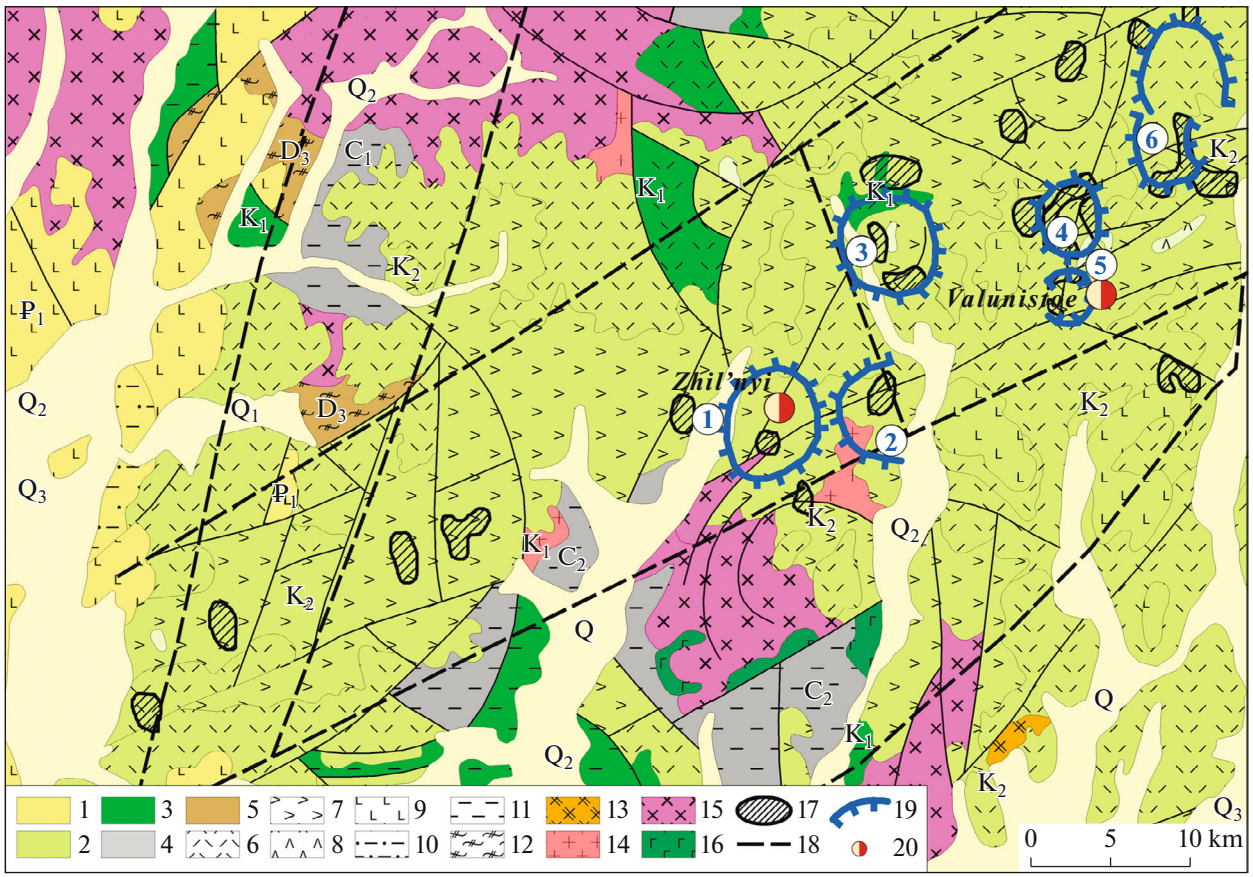

Fig. 2. Geological map of Amguema-Kanchalan volcanic field, compiled on basis of geological map, scale 1 : 200 000 (Sheets Q-60, XV, XVI) and (Romanov et al., 2002*). Legend: (1–5) age of rocks: (1) Early Paleogene, (2) Early Cretaceous, (3) Late Cretaceous, (4) Carboniferous, (5) Devonian; (6–9) volcanic rocks: (6) rhyolites, (7) dacites, (8) andesites, (9) basalts; (10) sandstones; (11) argillaceous shales; (12) metamorphic rocks; (13–16) intrusive rocks: (13) syenites and granosyenites, (14) granites and granodiorites, (15) diorites and monzonites, (16) gabbros; (17) subvolcanic rhyolite-dacite bodies; (18) large faults; (19) volcanic domes (structures) (1, Zhil'ninskaya, 2, Shakhskaya, 3, Oranzhevaya, 4, Valunistaya, 5, Shalaya, 6, Pravogornenskaya); (20) Au–Ag epithermal deposits.

(Fig. 2); in the geochemical field, they are emphasized by contrasting secondary dissemination aureoles of Au, Ag, Mo, and other accessory elements (Shabalin et al., 1993*). These structures confine several Au–Ag epithermal deposits (Valunistoe, Gornoe, and Zhil'noe) and promising ore occurrences (Ognennoe, Shakh, Oranzhevoe, and others).

The NE-trending Kanchalan fault zone is traced in the folded basement of volcanic rocks to a distance of 300–320 km. In the southwest, it is covered by Paleogene basalts, and on northeast it is traced to Amguema River (Romanov et al., 2002*). In the central part of the Kanchalan fault zone, which is the main ore-controlling structure in the area, is 12–30 km wide, with the general trend NE 65° (Fig. 2). All the revealed promising objects of Au–Ag formation are revealed within its limits.

Upper Cretaceous felsic rocks are the oldest units, which developed only in the northeastern part of the study area (Fig. 2). The volcanic section is topped by basalts, subalkaline basalts, and basaltic andesites with rare tuff interbeds. U–Pb ages obtained for volcanic and subvolcanic rocks of the Amguema-Kanchalan volcanic field range from 67.0 to 88.2 Ma (Sakhno et al., 2010).

Volcanogenic sequences of intermediate composition comprise gently sloping volcanic structures, as well as NE-oriented subsidence structures and swell-like domes (Fig. 2). Dip angles of layers are no more than 30°, or 20° for Paleogene effusive rocks. The most widespread are basaltic andesite and basalt dikes, which are hosted in Upper Cretaceous strata. Less developed are dacite and rhyolite–dacite dikes characteristic only for rocks of the Kytypnaivaam Formation (Romanov et al., 2002*).

Outcrops of the Paleozoic (Lower Carboniferous) highly metamorphosed carbonate sequence have been reported in the area 30 km west and southwest of the Valunistoe deposit (Fig. 2). Valanginian polymictic sandstones, limestones, and shales (carbonaceous–argillaceous and carbonaceous) overlie Paleozoic

rocks with an angular unconformity (Romanov et al., 2002*).

The most extensive and uninterrupted faults have northeastern trends coinciding with the general direction of volcanic structures (Fig. 2). Vertical offsets on them are more than 400 m. The faults are often accompanied by thick linear brecciation zones where fragments of host rocks are cemented by reddish brown premineral quartz. Based on particular trenches, the widths of brecciation zones are up to 100 m. Brecciation zones normally have clear contacts with the host rocks (Romanov et al., 2002*).

Later submeridionally trending faults partition the deposit area into a number of finer blocks characterized by different degrees of relative displacements, causing different degrees of erosion in blocks. Submeridional faults are accompanied by basaltic dikes and quartz veins up to 300 m long. Displacements of the earlier NE-trending faults along the later submeridional faults are up to 10 m or more in amplitude (Romanov et al., 2002*).

GEOLOGICAL FEATURES OF THE DEPOSIT

According to modern ideas, the Valunistoe ore field, 26 km^2 in area, spatially coincides with the Valunistaya and Shalaya volcanic domes, which approach each other (Fig. 2) and are located in the superintrusive part of the Leurvaam massif of the Late Cretaceous granodiorite–granite–leucogranite complex (Shabalin et al., 2006*).

The Valunistaya volcanic dome, 4 km in diameter, is rounded in plan view and confined by a ring fault (Fig. 2). In the section of OChVB volcanic rocks making up this dome, rocks (up to 650–800 m thick) attributed to the Amgen' sequence of the Ekitykin and Leurvaam formations have been revealed. Volcanic rocks demonstrate generally periclinal bedding; dip angles vary broadly (30°–50°) due to near-fault dislocations (Shabalin et al., 1995*).

Subvolcanic units of the Leurvaam complex (79.9 Ma; Sakhno et al., 2010) occupy at least 30% of the dome's surface (Fig. 3) and are found in its framing. The predominant among them are trachyrhyodacites of the Leurvaam complex. Multiple radial and through faults with different trends (northwestern, sublatitudinal, submeridional) resulted in the mosaic structure of the dome (Fig. 3). The offsets for particular blocks range from several to 200–300 m (Shabalin et al., 1995*).

Most commonly represented at the deposit are volcanic rocks of the Ekitykin Series (Fig. 3), which are highly various: ignimbrites, lavas and tuffs, tufobreccias ranging from rhyolitic to basaltic, lenses and interbeds of sedimentary rocks, subvolcanic bodies and dikes of andesites, basalts, and dacites (Fig. 4).

Deposition of vein and ore minerals at the deposit was preceded by the formation of explosive breccia from sharply angular fragments of host rocks, cemented by earlier fine-grained nonore quartz (Fig. 4b). Virtually all orebodies are accompanied by breccias (Shabalin et al., 2006*).

Ore-bearing hydrothermal units are represented by steeply dipping quartz and quartz–adularia veins localized in intensive metasomatic alteration zones, which developed along faults of different types and orientations. The thickness of vein zones ranges from several to several tens of meters. Along strike, they consist of several en echelon structures of different length. The thickness of particular veins in these zones varies from 0.1 to 24.7 m, with veins up to 1 m thick predominating; lengths of veins vary from 30 to 400 m. The majority of veins at the deposit are accompanied by shatter and brecciation zones. In some portions, quartz veins are separated by an interval (up to 10 m) of undisturbed host dacites, suggesting their noncoeval formation. Vein contacts are normally clear. The veins are ubiquitously accompanied by multiple apophyses. Ores of the Valunistoe deposit are complex gold–silver. The correlation coefficient for Au and Ag is 0.85 which is relatively high (Shabalin et al., 1995*).

Judging from the absolute age of adularia (Leier et al., 1997; Newberry et al., 2000), the formation time of orebodies at the Valunistoe deposit is the Late Cretaceous (79 ± 2 Ma), synchronous to the eruptions of plateau basalts that screened hydrothermal fluids.

In the area of the Valunistoe ore field, 12 ore-bearing vein zones are revealed (Shabalin et al., 1995*), of which studied in the most detail are the Main and New (Fig. 3).

(1) The *Main vein zone* is traced in a northeastern direction to the distance of 1600 m; its width is 40–80 m, with a steep (70°–85°) SSE dip. The majority of veins in the Main zone are localized within the limits of a complex-shaped subvolcanic body of fluidal rhyodacites (Fig. 3). The veins are grouped in four en echelon units consisting of one to three main veins accompanied by short subparallel and branching veins. Thickness of main veins ranges from 0.6 to 11.0 m, while their lengths vary from 200 to 540 m; branching veins are 0.2–2.0 m thick and 50–200 m long (Shabalin et al., 1995*, 2006*). Compound veins in open fissures with parallel sharp contacts predominate. Metasomatic veins with curved indistinct contacts are rarely encountered. The strike and dip of these veins coincide with that of the entire Main vein zone.

Mineralization in veins in inhomogeneous. Au and Ag contents are 0–474 and 0–3794 g/t, respectively (based on sampling data). The maximum Au and Ag contents in veins, based on float sampling of bonanzas, are 1969 and 22108 g/t, respectively (Shabalin et al., 2006*). In hydrothermally altered rocks which host ore veins, Au and Ag contents are less than 0.5 and 10 g/t, respectively, only in some parts they can increase up to few grams per ton for Au and few tens of grams for Ag. Au/Ag ratio in orebodies of the Main vein zone changes from 1 : 65 to 10 : 1, while its average

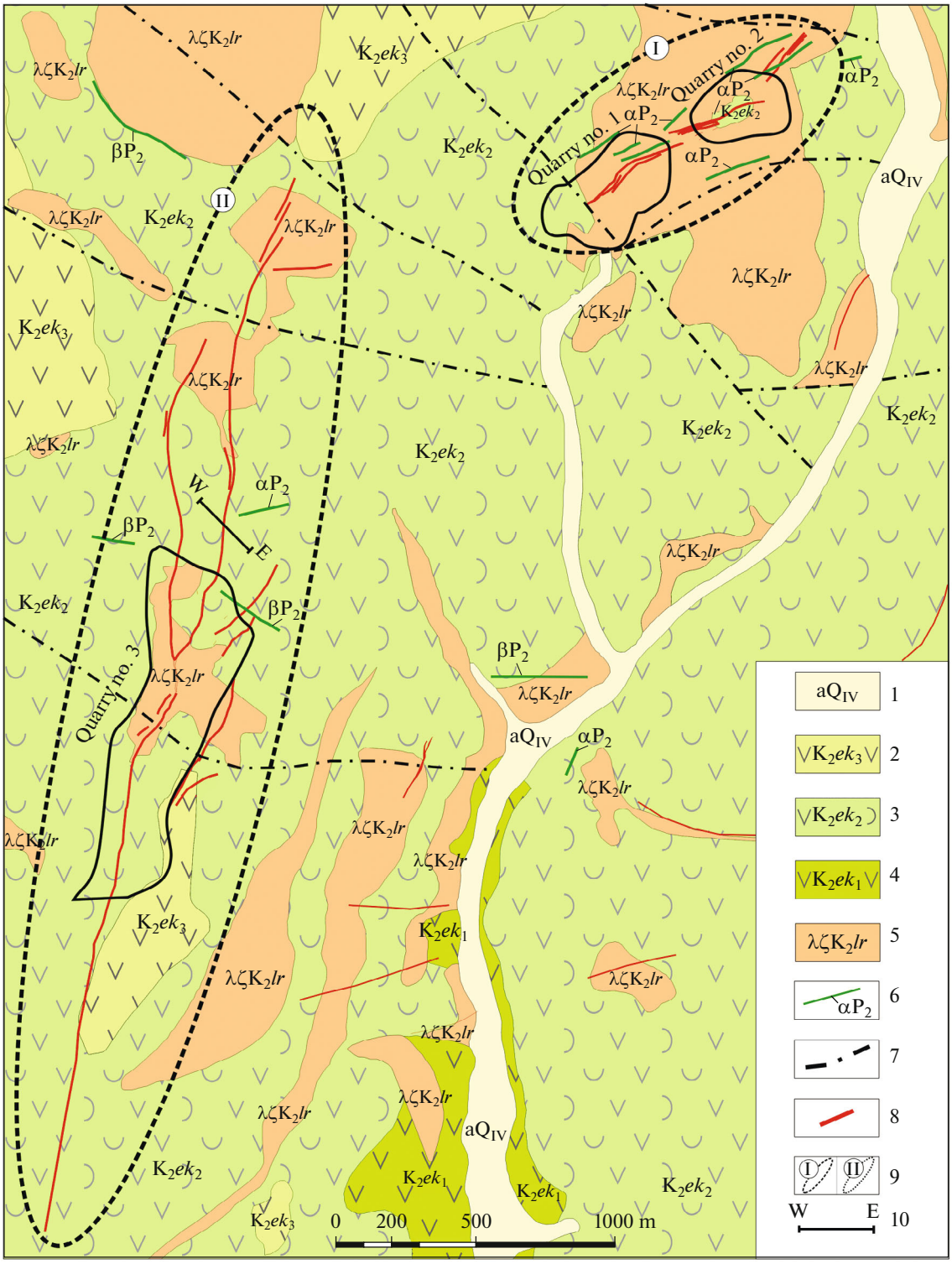

Fig. 3. Schematic geological map of Valunistoe deposit (after data of Anadyr Geological Survey Expedition and Valunistyi mine). Legend: (1) modern deposits (alluvial pebbles, boulders, gravels, sands, and loamy sands); (2–4) Ekitykin Formation: (2) upper sequence (andesites, andesite-basalts with thin tuff interbeds containing carbonized detrital material), (3) middle sequence (uneven-sized clastic tuffs of intermediate composition), (4) lower sequence (tuffaceous sandstone, andesites, basalts, thin interbeds of ash tuffs); (5) Leurvaam subvolcanic complex (rhyolite and rhyodacites bodies); (6) Il'myneiveyem subvolcanic complex (bodies and dikes of andesibasalts, andesites, and basalts); (7) faults; (8) productive quartz–adularia veins; (9) contours of Main (I) and New (II) vein zones; (10) position of section shown in Fig. 5; OB 14, orebody no. 14.

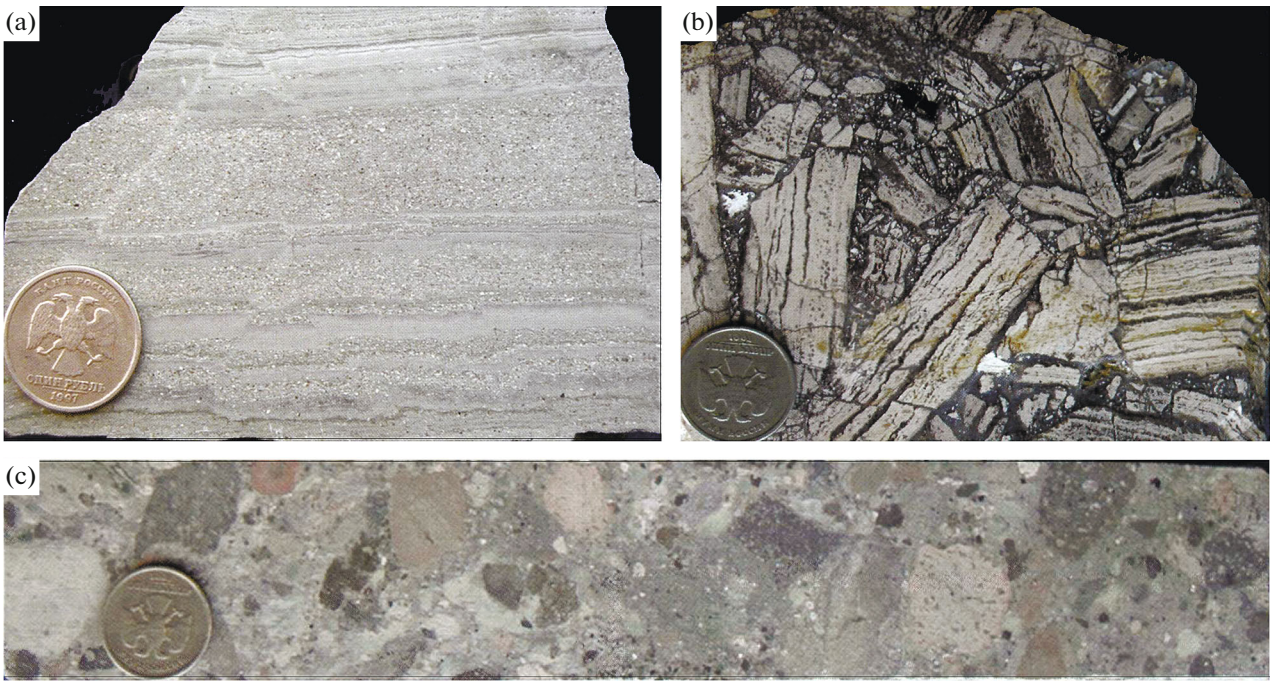

Fig. 4. Host rocks of Valunistoe deposit (Magadannedra Geological Museum, I.S. Raevskaya's collection): (a) finely bedded tuffs, trench 175; (b) pre-mineral hydrothermal breccia with fragments of fluidal-banded rhyolites cemented with pyrite–quartz material, New vein zone, trench 113; (c) tuffaceous breccia with fragments of rhyolites and andesites, Main vein zone, well 91.

value is 1 : 10. Average fineness of native gold is 600‰, with its units ranging in size from 0.01 to 2 mm, rarely larger.

(2) The *New vein zone* is traced in a meridional direction by 850 m; its length is 1500 m and its thickness is 100–200 m (Fig. 3). It consists of a series of closely located parallel quartz, less often adularia–quartz veins of 0.2–0.9 to 5–8 m thick and up to 500–600 m long. The New vein zone is marked in secondary dissemination aureoles with contrasting anomalies of up to 10 g/t for Au and 50 g/t for Ag (Shabalin et al., 2006*). The ranges of Au and Ag contents in veins are 3.4–135.7 and 33.0–1238.2 g/t, respectively. Veins dip steeply (70°–85°) to the west (Fig. 5). Based on drilling data, the vertical extent of mineralization is up to 200 m (Fig. 5).

METASOMATIC ALTERATIONS OF HOST ROCKS

Among metasomatic alterations, two types are especially distinct: the first is represented by low- to medium-temperature propylitization on tuffolavas of porphyry andesites, while the second is K-feldspathization. Zones of metasomatic K-feldspar development have no sharp boundaries, gradually being replaced with sericitized rocks. K-feldspar is represented by solid fine-grained adularia aggregates associated with quartz in the inner zone and sericite in the outer. Near-vein adularization is a relatively local process that is not reported at distances greater than 10 m from veins.

Propylites of the Valunistoe deposit are attributed to the epidote–chlorite facies (Fig. 6a) and, to a lesser degree, to low-temperature chlorite–albite (Fig. 6b), manifested in the upper parts of the section. Table 1 gives the compositions of epidotes. It should be noted that a common characteristic feature of propylites is the absence or very limited presence of metasomatic calcite. Based on the microprobe analysis and diffractometry data, chlorites from propylites (Fig. 6b) can be attributed to clinochlore (Table 2).

According to the data of microprobe and optical analyses, all plagioclases in the studied samples are replaced with albite of no higher than nos. 8–10 and the CaO content in them is no more than 0.56 wt %. Albitized plagioclase is ubiquitously and intensively replaced with K-feldspar, often to the appearance of complete pseudomorphs. Newly formed K-feldspar is represented by an almost pure potassic variety (the Na_2O content is no more than 0.25 wt %).

The replacement of propylite-hosted albite with K-feldspar approaching the surface and decreasing temperature has been repeatedly described in the geological literature (see, e.g., (Rusinov, 1989) and others). Many authors emphasize that K-feldspathization often coincides with fault-related highly permeable zones (Naboko and Glavatskikh, 1970; Keite et al., 1978).

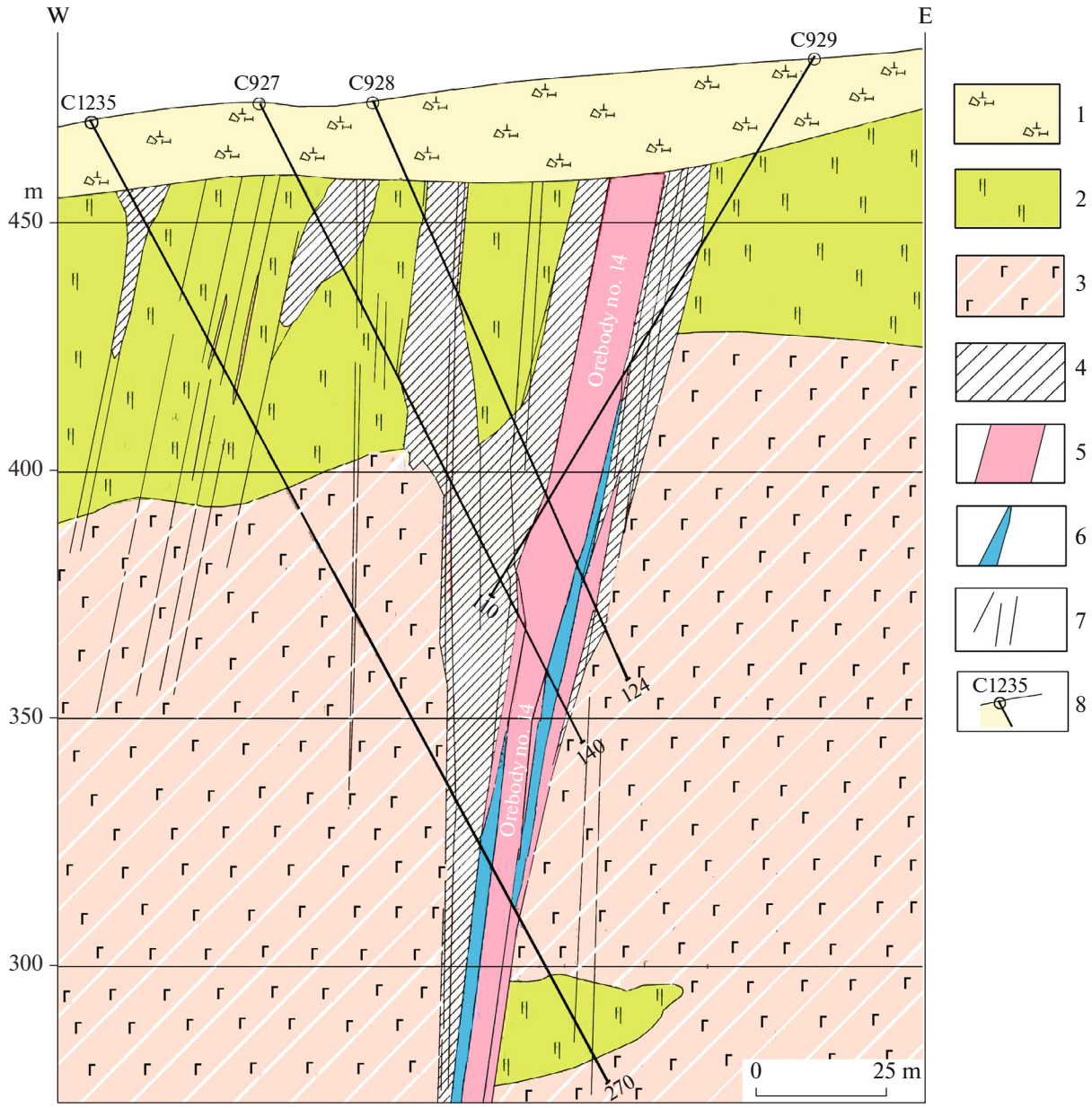

Fig. 5. Geological section across trend of orebody no. 14 in New vein zone (after data of Anadyr Geological Survey Expedition and Valunistyi mine). (1) Quaternary deposits (prolivial-deluvial loamy sands and rock waste); (2) Upper Cretaceous Ekitykin Formation, lower sequence: tuffaceous sandstone, andesites, basalts, ash tuffs (up to 200 m); (3) Upper Cretaceous rhyodacites of Leurvaam subvolcanic complex; (4) near-vein adularization and sericitization; (5) orebody no. 14 (quartz–adularia vein); (6) calcite vein; (7) secondary faults; (8) coring wells.

Later sericitization and argillization were overprinted on propylites (Figs. 6c–f); their zones are ubiquitously crosscut by sulfide-bearing quartz–adularia veinlets (Fig. 6e). Notably, veinlet adularia remains completely unaffected by sericitization (Fig. 6e), which suggests its later origin with respect to metasomatic K-feldspar in the host rock (Fig. 6d).

Sericitization, which refers to a type of acid metasomatism, is an integral part of the general hydrothermal cycle at all Au–Ag deposits in volcanic rocks (see (Rusinov, 1989) and others). A peculiarity of the Valunistoe deposit is relatively weak development of sericite metasomatites, which are sporadic and do not demonstrate any relationship with the ore mineralization. It is only clear that they preferably develop on felsic volcanics.

Argillization processes obviously developed later than the main vein mineralization. Fine kaolinite clusters are often observed in quartz and quartz–adularia ore veins (the presence of this mineral is supported by

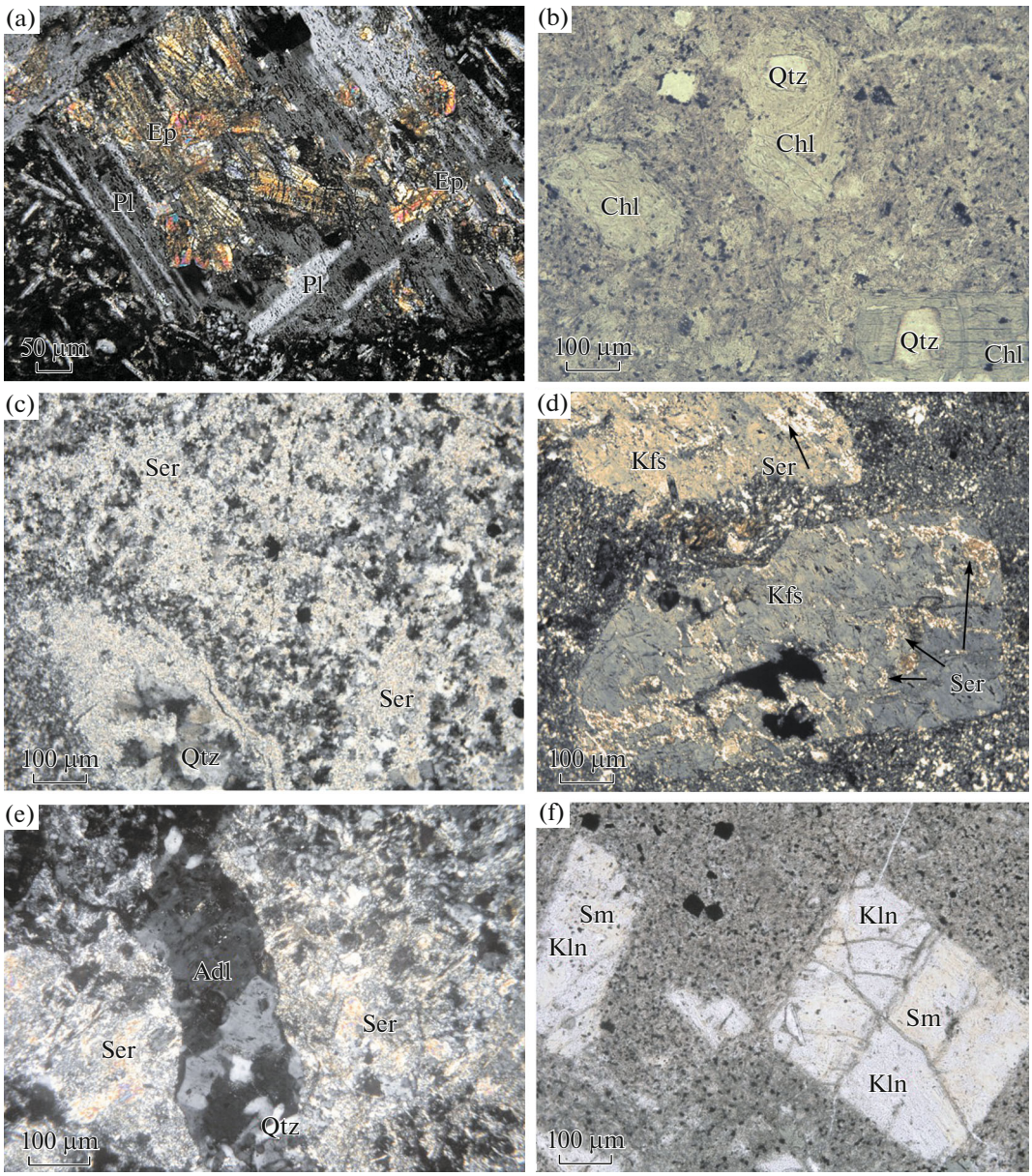

Fig. 6. Microimages of metasomatic rocks of Valunistoe deposit: (a) forms of metasomatic epidote development in plagioclases of propylitized basalts, crossed nicols; (b) metasomatic chlorite that completely replaced impregnations of dark-colored minerals and, partially, groundmass of basaltic andesite, parallel nicols; (c) quartz–sericite aggregate without initial rock relics, crossed nicols; (d) replacement of K-feldspar impregnations with sericite, crossed nicols; (e) nonsericitized quartz–adularia veinlet in propylite; (f) replacement of feldspars with kaolinite and smectite. Qtz—quartz; Kfs—K-feldspar in pseudomorphs after plagioclase; Ser—sericite; Chl—chlorite; Ep—epidote; Pl—plagioclase; Adl—vein adularia; Sm—smectite; Kln—kaolinite.

X-ray diffractometry). In singular cases, intensive replacement of K-feldspars with clay minerals was reported (Fig. 6f).

It should also be noted that surface hypergene alterations are weakly manifested, judging from the good degree of preservation of the sulfide groundmass and the presence of goethite films and crusts around pyrite grains in quartz veins and host rocks revealed by trenching.

GEOCHEMICAL FEATURES OF ORES

The predominant component of Valunistoe deposit ores is SiO_2 (77.00–94.62%); there are significant concentrations of CaO (0.11–10.48), Al_2O_3 (1.23–2.07), K_2O (0.22–5.14), and Fe_2O_3 (0.14–1.37) (Table 3), and sometimes F (0.4–15.2). The ores are characterized by low and very low Na_2O, TiO_2, P_2O_5, and MnO contents. The sulfide content in the studied

Table 1. Chemical composition of epidote from host rocks of Valunistoe deposit (well)

Component	V-80	V-80	V-80
SiO_2	38.08	38.68	38.41
TiO_2	0.20	0.06	0.17
Al_2O_3	20.99	25.53	22.25
FeO_{total}	15.41	9.83	14.68
MnO	0.07	0.12	0.05
CaO	23.32	23.36	22.94
H_2O	1.87	1.98	1.99
Sum	99.94	99.56	100.19
Coefficients in crystallochemical formulas			
Si	3.05	3.05	3.06
Al	1.98	2.37	2.09
Ca	2.01	1.98	1.96
Ti	0.01	0.01	0.01
Fe	0.93	0.58	0.86
O	1.00	1.00	1.00
OH	1.00	1.04	1.06

Mineral formula is $Ca_2(Al, Fe)_3[SiO_4][Si_2O_7]O(OH)$.

ores is low (S_{total} = 0.07–1.25%), which is typical of epithermal mineralization (Sidorov, 1978).

The ores are enriched in quite many elements (Au, Ag, Sb, Cd, Pb, Cu, Zn, Se, Mo, Te, and Cr) (Table 4, Fig. 7) compared to the mean values for the upper crust (Taylor and McLennan, 1985), ranging from severalfold (Se, Mo, Te, and Cr), to tenfold (Cd, Pb, Cu, and Zn) and hundredfold (Sb), reaching an excess of tens and hundreds thousand times for Au and Ag (Fig. 7). This indicates a geochemical relationship between certain trace elements and their synchronous role in mineralization. Judging by the data from Table 5 and Fig. 8, light "hydrophile" cerium group REE are predominant in the studied ores and host rocks (Zharikiov et al., 1999; Mineev, 1974).

The host rocks are mainly represented by basalts and trachydacites, which are often brecciated and cut by various veinlets. They are characterized by a negative anomalous REE distribution (Fig. 8b), with relatively close $\sum REE_N$ values (180–531), but with considerably more varied Eu/Sm_N values (0.53 to 1.2) (Table 6).

Samples from explosive breccias consist of fragments belonging to various rocks, in particular, basalts, basaltic andesites, trachydacites, trachydacites, etc.; the fragments are often sharply angular, cemented with finely abraded material and quartz; they are also cut by thin gypsum veinlets. They are characterized by a negative distribution of lanthanides, high $\sum REE_N$ values (170–439), and a negative Eu anomaly (Table 6, Fig. 8e).

Samples from veins of various composition (adularia–quartz–calcite and fluorite–quartz–calcite to highly calcite) are characterized by gold contents ranging from background to several grams per ton, with low (background) concentrations of silver. Note that ore samples represented by complex breccias (sample V-71) ore basaltic andesites with multiple adularia–quartz and fluorite–quartz veinlets (sample V-78) have high $\sum REE_N$ values (99–298), a negative lanthanide distri-

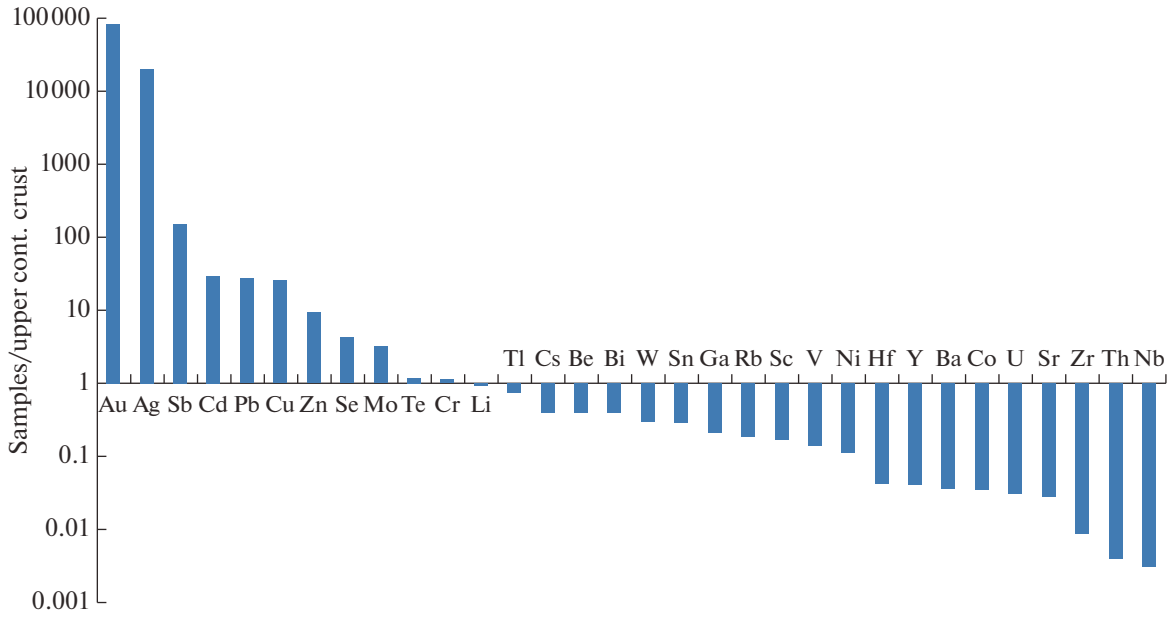

Fig. 7. Distribution of main trace elements in epithermal Au–Ag ores of Valunistoe deposit, normalized to average values for upper crust (Taylor and McLennan, 1985).

Table 2. Chemical composition of chlorite (wt %) from host rocks of Valunistoe deposit (Russian Northeast)

Component	V-80	V-80	V-80	V-78	V-78	V-78
SiO_2	27.77	28.56	28.19	31.35	32.30	33.34
TiO_2	0.02	0.00	0.00	0.01	0.00	0.02
Al_2O_3	18.91	18.94	19.13	17.48	17.92	18.40
FeO_{total}	23.30	24.91	24.29	20.22	21.12	20.05
MnO	0.73	0.81	0.93	0.90	0.68	0.83
MgO	16.34	16.25	16.15	15.05	17.55	16.74
CaO	0.06	0.06	0.07	0.25	0.20	0.25
Na_2O	0.00	0.03	0.00	0.02	0.03	0.02
Cr_2O_3	0.04	0.01	0.05	0.18	0.15	0.34
H_2O	11.19	11.21	11.20	9.96	10.44	10.07
Sum	98.42	100.81	100.11	95.59	100.53	100.19
Coefficients in crystallochemical formulas						
Si	2.93	2.95	2.94	3.40	3.29	3.41
Al^T	1.06	1.04	1.06	0.59	0.70	0.59
Total T	4.00	4.00	4.00	4.00	4.00	4.00
Al^A	1.29	1.26	1.29	1.64	1.45	1.62
Fe	2.06	2.16	2.12	1.84	1.80	1.71
Mg	2.58	2.51	2.51	2.44	2.67	2.55
Mn	0.06	0.07	0.08	0.08	0.06	0.07
Ca	0.01	0.01	0.01	0.03	0.02	0.03
Na	–	0.01	–	–	0.01	–
Total A	6.01	6.01	6.01	6.03	6.01	5.00
OH^-	7.75	7.77	7.76	6.89	7.23	6.97
O^{2-}	0.25	0.23	0.24	1.10	0.77	1.03
$Fe_{total}/(Fe_{total} + Mg)$	0.44	0.46	0.46	0.43	0.40	0.40

bution, and subchondrite values of the Eu/Sm_N ratio, 0.62–0.9 (Table 6; Figs. 8c, 8f, 8g).

Veins where calcite is predominant and Au contents are anomalous significantly differ in the level of REE contents and character of the REE distribution (Fig. 8g). Vein breccias containing significant amounts of fragments of altered host rocks have higher ∑REE values (up to 293), a negative REE distribution, and subchondrite values of the Eu/Sm_N ratio (Table 6). Their relatively pure units differ in very low $\sum REE_N$ values (2.1–33.0) and approximately equal contents of light and heavy lanthanides, with a relatively low level of intermediate ones (Table 6). We emphasize the presence of positive Eu anomalies typical of rich ore samples from adularia–quartz veins (Fig. 8g).

At the Valunistoe deposit, we found samples demonstrating predominance of Y over LREE or approximately equal contents; they mostly correspond to veins of quartz–calcite or a highly calcite composition with a subchondrite lanthanide distribution (Fig. 8g).

Thus, the obtained data indicate relatively similar REE distributions for the majority of veins and host rocks. In the latter case, this is primarily caused by a relatively high REE content in the host rocks with a characteristic negative distribution with values ranging from those corresponding to chondrite to negative Eu anomalies, depending on the chemical compositions of rocks.

STRUCTURAL-TEXTURAL PECULIARITIES OF QUARTZ VEINS

In ore-bearing quartz veins of the Valunistoe deposit, we established broadly developed breccia, geode–breccia, brecciform, framed-platy, rhythmically banded (taxitic), and colloform-zonal structures typical of near-surface mineralization (Figs. 9a–c).

Geode–breccia structures are predominant in veins. Small quartz druses are developed in small cavities. Axial parts of veins sometimes occupy veinlets of drusoid amethyst of up to 6 cm thick. Less often, ame-

Table 3. Chemical composition of ores (wt %) of Valunistoe deposit

Sample nos.	SiO_2	TiO_2	Al_2O_3	Fe_2O_3 total	MnO	MgO	CaO	Na_2O	K_2O	P_2O_5	S total	Σ
V-20	86.07	<0.02	1.23	0.14	0.025	0.04	10.48	0.09	0.47	<0.02	0.25	98.8
V-22	86.00	<0.02	<0.02	0.20	0.006	<0.02	0.06	<0.02	5.14	<0.02	0.07	91.4
V-23	93.00	0.05	<0.02	0.48	0.058	<0.02	0.11	<0.02	2.53	0.02	0.15	96.4
V-24	77.00	0.07	<0.02	1.00	0.074	<0.02	4.37	<0.02	5.74	<0.02	0.45	88.7
V-75	78.80	0.00	<0.02	0.07	0.058	<0.02	14.92	<0.02	0.22	0.00	0.02	94.0
V-1	87.06	0.01	3.60	0.45	0.04	0.13	0.07	0.09	0.90	<0.02	0.52	92.8
V-2	92.79	0.01	1.92	1.37	0.03	0.14	0.03	0.09	0.33	0.02	1.25	97.9
V-3	94.24	0.01	2.07	0.94	0.04	0.13	0.02	0.09	0.36	0.02	0.78	98.7
V-4	94.62	0.02	2.03	0.91	0.04	0.13	0.02	0.09	0.36	0.02	0.74	98.9
C_a	92.17	0.01	2.40	0.91	0.04	0.13	0.035	0.09	0.49	0.02	0.82	97.1

C_a, average content. Samples V-1,V-2, V-20, V-22, V-23, and V-24 are from Main vein zone; V-3, V-4, and V-75, from New vein zone.

thyst veinlets are observed immediately in hydrothermally altered rocks.

Earlier fine-grained and cryptocrystalline quartz in veins (sometimes chalcedonic with zones of nucleating coarse-grained pennant quartz) is changed to larger units. In this respect, we revealed no visible intercepts with the subsequent variety of coarse-grained quartz, since the separation between these two generations (fine- and coarse-grained) is not sufficiently clear.

We found multiple dark-colored zonally or sometimes sectorially arranged microinclusions in coarse-grained radial-fibrous, spherulitic, and pennant quartz (Fig. 9e). The majority of these microinclusions are likely gaseous–liquid, although small interpositions of ore minerals are also present, imparting an inhomogeneous haziness to quartz. The temporal relationships between spherulitic and pennant quartz suggest that the former variety most likely appeared earlier.

Unevenly grained (with a rhombic cross section) and xenomorphic adularia forms segregations subcoeval to quartz, but sometimes it can also found in selvages of thin quartz veinlets. After the appearance of adularia, cataclasis and intravein shattering are observed (Fig. 9f).

Note that parts of veins enriched in Au and Ag usually demonstrate greater or lesser signs of metacolloid structures at the macroscopic and microscopic levels, while ore minerals coincide with bands of cryptocrystalline quartz and adularia aggregates, which are visible in samples due to their gray color and orientation in parallel to banding (Fig. 9c).

MINERALOGICAL FEATURES OF ORES

The main vein ore minerals of the deposit are quartz and adularia that together make up 98–99% of the vein mass. Although the amount of adularia alone is rarely more than 5–7%, it can be up to 30% and more in places. Less frequently encountered minerals are calcite, chlorite, fluorite, sericite, pyrophyllite, kaolinite, montmorillonite, gypsum, and epidote. Chlorite (up to 3–5%) was reported at middle and lower depth levels of orebodies and is not characteristic of the upper level.

An important mineralogical feature is the broad development of late vein minerals (calcite, fluorite, and gypsum). Notably, gypsum occurrences clearly tend to near-surface mineralization levels, while large-crystalline calcite and fluorite are intensively developed below here in quartz veins.

The Au and Ag distributions in orebodies are highly inhomogeneous, with a pocket nature. The amount of ore minerals in veins is usually no more than 0.5%, rarely up to 5%. Ore minerals are represented by native gold (electrum), pyrite, chalcopyrite, acanthite, native Ag, aguilarite, stromeyerite, Ag sulfosalts, and, in abruptly subordinate amounts, galena and sphalerite. Ore mineralization can be found (1) in colloform adularia–quartz bands, (2) in adularized fragments of wall rocks, (3) in adularia crusts, (4) at the boundaries of adularia and quartz clusters, and (5) in metasomatically altered rocks.

At the lower horizons of veins (100 m depth from the surface), the roles of chalcopyrite, galena, and sphalerite increase (Shabalin et al., 1995*). In sphalerite, emulsive impregnation of chalcopyrite occurs (notably, it is absent in the upper horizons of veins). Gold–acanthite mineralization at depth changes to gold–chalcopyrite. A peculiarity of ores is that mineral forms of gold are variable, Se mineralization is uniformly distributes, and Ag and Bi sulfosalts are present.

More than 50 minerals have been identified up to now in ores and host rocks of the studied sites (Table 7), taking into consideration the results of earlier investigations (Bryzgalov and Krivitskaya, 1998; Novoselov

Table 4. Representative ICP-MS analyses (g/t) of Valunistoe deposit ores

Element	Valunistoe (g/t)					
	V-1	V-2	V-3	V-4	AM	GM
Li	131.6	10.7	8.5	9.6	40.101	18.420
Be	2.0	0.83	0.92	1.1	1.218	1.141
Sc	2.9	1.9	1.5	1.3	1.910	1.820
V	5.0	9.1	10.5	9.5	8.514	8.195
Cr	49.5	45.8	30.3	35.5	40.253	39.495
Co	0.46	0.32	0.30	0.30	0.345	0.340
Ni	2.1	1.5	4.6	1.6	2.432	2.180
Zn	562	1020	672	579	708.102	687.088
Ga	6.4	2.8	2.7	3.1	3.757	3.502
As	BDL	BDL	BDL	BDL	0.000	0.000
Se	2394	137	89.3	71.7	672.991	213.944
Rb	29.0	18.6	17.0	19.8	21.103	20.648
Sr	26.8	6.7	6.4	7.1	11.760	9.521
Y	1.3	0.80	0.72	0.85	0.910	0.888
Zr	7.2	0.65	1.6	1.0	2.615	1.649
Nb	0.053	0.066	0.087	0.11	0.078	0.076
Mo	4.3	5.7	4.3	5.7	4.992	4.943
Ag	28070	3561	2463	1284	8844.500	4216.586
Cd	9.2	2.8	1.8	1.8	3.876	2.999
Sn	0.4	2.9	2.5	2.4	2.023	1.567
Sb	15.4	37.7	36.3	39.4	32.197	30.192
Te	5.0	BDL	BDL	BDL	1.252	1.496
Cs	2.8	1.1	1.1	1.3	1.557	1.431
Ba	58.5	13.8	13.9	15.0	25.300	20.267
La	2.6	0.69	0.78	0.89	1.244	1.059
Ce	9.7	1.1	1.2	1.4	3.359	2.076
Pr	1.2	0.12	0.13	0.15	0.401	0.232
Nd	4.5	0.47	0.53	0.60	1.537	0.911
Sm	0.79	0.088	0.104	0.108	0.272	0.167
Eu	0.09	0.046	0.057	0.063	0.065	0.063
Gd	0.46	0.080	0.075	0.093	0.177	0.126
Tb	0.062	0.013	0.028	0.019	0.030	0.026
Dy	0.30	0.093	0.11	0.12	0.156	0.139
Ho	0.047	0.030	0.021	0.034	0.033	0.032
Er	0.15	0.075	0.072	0.11	0.100	0.096
Tm	0.016	0.008	BDL	0.0083	0.008	0.032
Yb	0.10	0.053	0.063	0.070	0.071	0.069
Lu	0.013	BDL	0.009	0.008	0.008	0.031
Hf	0.33	BDL	0.03	0.06	0.105	0.155
Ta	BDL	BDL	BDL	BDL	0.000	0.000
W	0.65	0.59	0.54	0.61	0.598	0.597
Tl	0.5	0.6	0.5	0.6	0.545	0.544
Pb	654.5	707.6	480.3	396.0	559.598	544.785
Bi	0.31	0.024	0.022	0.033	0.098	0.048
Th	0.065	0.023	0.042	0.046	0.044	0.041
U	0.28	0.069	0.050	0.051	0.112	0.084
Au	1936	17.4	8.2	6.5	491.987	36.682
Cu	2461	500	391	375	931.753	651.841

BDL, below detection limit; AM, arithmetic mean; GM, geometric mean. Samples V-1 and V-2 are from Main vein zone; V-3 and V-4, New vein zone.

Table 5. Indicative parameters and ratios for epithermal ors of Valunistoe deposit

Parameters and ratios	Samples										
	V-1	**V-2**	**V-3**	**V-4**	**V-20-a**	**V-20-c**	**V-22-a**	**V-22-c**	**V-23**	**V-24-a**	**V-24-c**
∑REE	20.03	2.86	3.18	3.67	51.10	99.38	1.93	2.87	8.88	77.77	75.28
∑LREE	18.88	2.51	2.80	3.21	42.81	88.92	1.69	2.42	8.07	66.01	66.13
∑HREE	1.15	0.35	0.38	0.46	8.29	10.46	0.24	0.45	0.81	11.76	9.15
∑LREE/∑HREE	16.44	7.14	7.41	6.94	5.16	8.50	7.07	5.36	9.98	5.61	7.23
Hf/Sm	0.42	0.00	0.29	0.55	0.00	0.00	0.00	0.00	0.00	0.00	0.00
Nb/La	0.02	0.09	0.11	0.12	0.00	0.00	0.00	0.00	0.00	0.00	0.00
Th/La	0.02	0.03	0.05	0.05	0.00	0.00	0.00	0.00	0.00	0.00	0.00
Y/Ho	27.66	26.66	34.28	25.00	31.10	30.36	15.86	17.18	21.48	18.59	25.23
U/Th	4.31	3.00	1.19	1.11	0.00	0.00	0.00	0.00	0.00	0.00	0.00
Rb/Sr	1.08	2.77	2.65	2.79	0.33	0.15	4.45	5.47	1.45	1.72	1.24
Sr/Ba	0.45	0.48	0.46	0.47	0.64	1.39	0.22	0.09	0.27	0.21	1.00
Zr/Hf	21.81	DL	53.33	16.66	DL	DL	DL	DL	DL	DL	DL
Co/Ni	0.21	0.21	0.06	0.18	DL	DL	DL	DL	DL	DL	DL
Te/Se	0.00	DL	DL	DL	0.00	0.00	0.00	0.00	0.00	0.00	0.00
Au/Ag	0.06	0.00	0.00	0.00	0.99	0.99	2.66	0.60	0.00	0.13	0.34
Cu/Mo	572.32	87.71	90.93	65.78	176.60	15.20	67.00	86.28	23.71	14.40	4.20
Pb/Nd	145.44	1505.53	906.22	660.00	2.61	0.49	1246.16	328.90	120.48	2.17	DL
Eu/Eu*	0.562	1.505	1.342	1.565	0.676	0.644	7.797	6.989	1.288	1.072	0.672
Ce/Ce*	1.74	0.83	0.80	0.83	1.34	1.55	0.97	1.01	1.03	1.11	1.07
LaN/YbN	17.66	8.84	8.41	8.63	6.61	9.13	23.51	31.11	39.27	5.79	7.49
LaN/SmN	2.05	4.89	4.68	5.14	1.26	1.44	3.68	1.81	3.31	1.96	2.88
GdN/YbN	3.72	1.22	0.96	1.07	4.68	4.50	6.15	26.73	10.04	2.88	1.82
LaN/LuN	20.75	DL	8.99	11.54	8.31	10.96	4.23	3.96	18.57	6.23	6.56
∑Ce	18.00	2.38	2.64	3.04	39.54	83.43	1.35	1.82	7.61	61.13	62.54
∑Y	1.74	0.35	0.39	0.43	9.70	13.54	0.49	0.96	1.09	13.39	9.79
∑Sc	0.27	0.13	0.14	0.19	1.85	2.39	0.08	0.09	0.16	3.24	2.94
Eu/Sm	0.11	0.52	0.54	0.58	0.18	0.15	4.78	4.14	0.39	0.32	0.18

Eu/Eu* = EuN/(SmN*GdN)0.5; Ce/Ce* = CeN/(LaN*PrN)0.5; LREE and HREE mean light and heavy REE, respectively; total contents are presented on REE groups (Mineev, 1974), namely, cerium (ΣCe), yttrium (ΣY), and scandium (ΣSc). DL means detection limit.

et al., 2009; Shabalin et al., 1995*). Of more than 30 hypogene ore minerals, about 20 (Au and Ag minerals) are of industrial interest. Below we briefly describe the main ore minerals.

Pyrite is inhomogeneously developed in the form of crystals and their aggregates, up to 0.1 mm in size; crystals are mainly corroded. As noted above, pyrite can contain microinclusions of native gold, as well as Ag sulfides and sulfosalts. In one sample we found a fine *galena* inclusion; in several cases, later-generation pyrite was found in the form of rims in the periphery of acanthite.

Chalcopyrite forms quite rare xenomorphic segregations predominantly several hundredths of a millimeter in size (Fig. 10a); it is also encountered as fine curved-shaped relicts replaced with acanthite. Sometimes very fine discontinuous bornite rims develop after chalcopyrite.

Sphalerite is represented by rare isometric inclusions a few hundredths of a millimeter in size, often at contacts with chalcopyrite, sometimes in aggregates with tetrahedrite (Fig. 10b).

Native gold is observed in chalcopyrite and pyrite, as well as in vein minerals (adularia, quartz, and fluorite), forming predominantly rounded isometric segregations (Fig. 10a), but also elongated ones of irregular shape. In one case, native gold was found in calcite. Additionally, limbate and more complex units of native gold are reported in aggregates with native silver. Segregations vary from 1 to 80 μm in size. Native gold is characterized by the elongated shapes of its units, with a higher fineness of up to 736, with the

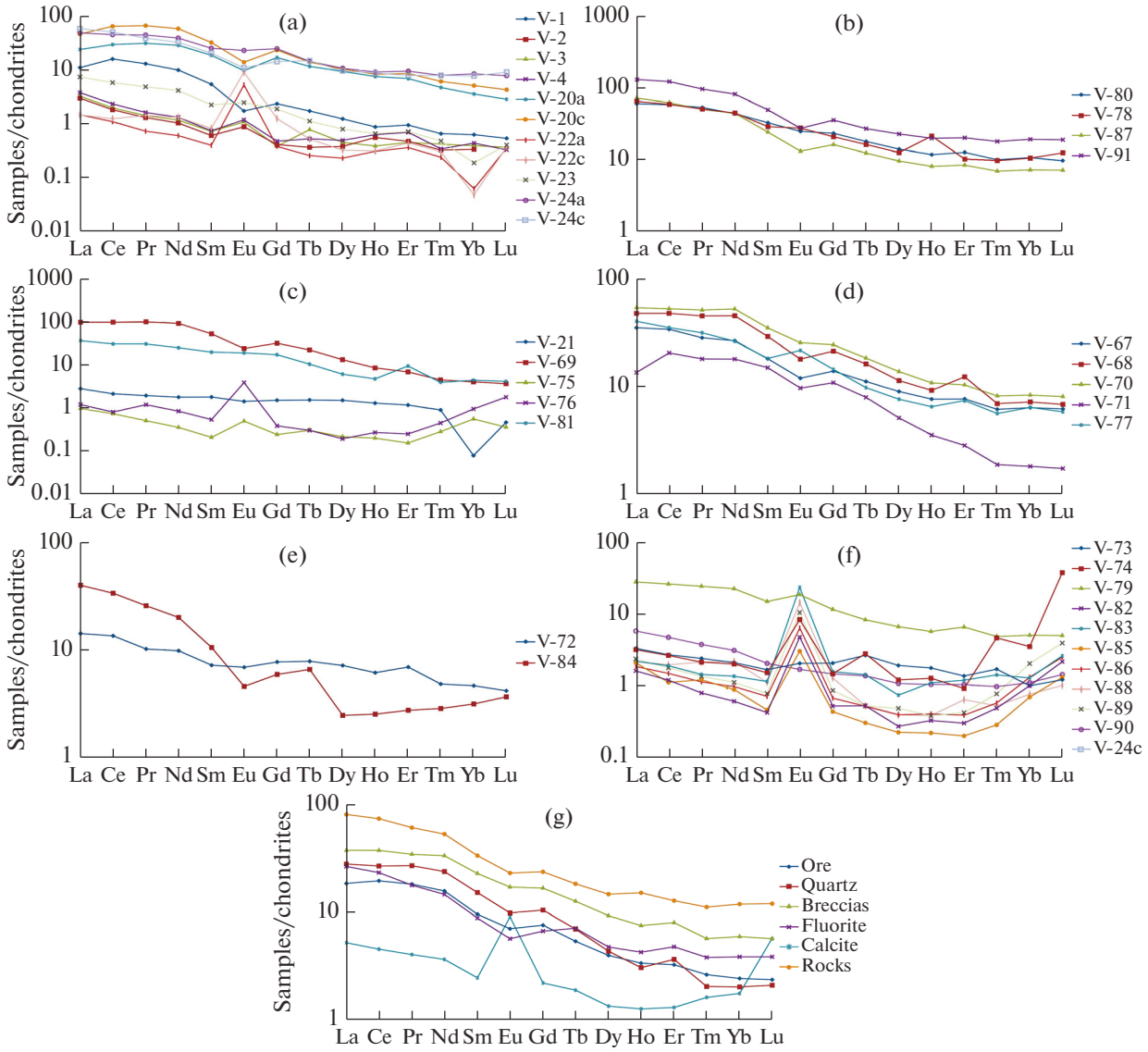

Fig. 8. Chondrite-normalized (Anders, 1989) REE distributions for different objects of Valunistoe deposit: (a) epithermal ores, (b) host rocks, (c) nonore quartz veins, (d) hydrothermal breccias, (e) fluorite, (f) calcite-bearing Au–Ag veins; (g) distribution of average REE values for aforementioned objects. Numbers of samples are provided in Tables 8–10.

average fineness for the entire set of available samples of the Valunistoe deposit being 608 (the total variation range is from 588 to 736‰; Table 8). Sometimes it contains mercury (up to 7 wt %) and copper (0.04–0.80 wt %; Table 8).

Native silver is found in aggregates with chalcopyrite and naumannite within fluorite veinlets or at the contact between adularia or quartz and fluorite and within aggregates of Au and Ag minerals (Figs. 10b–10d). In abundance in the ores of this deposit, the native silver content is much less than that of native gold, because the former is localized only where fluorite occurs. The composition of native silver is presented in Table 8. As is seen from analyses, mercury content in it ranges from 5.6 to 11.8 wt %, with admixtures of Cu (0.13–0.58 wt %) and Bi (0.30–0.35 wt %) (Table 8). Segregations of native silver can have both clear and fuzzy contacts with native gold; they are isometric in shape and 10–100 μm in size (Figs. 10b–d). The fineness of native silver varies from 0 to 377‰ (Table 8).

Naumannite (Ag_2Se) is found in two cases, within the limits of chalcopyrite segregations confined in fluorite or at the contact between fluorite and adularia or quartz. Its segregations are no more than 12 μm in size. The composition of naumannite is presented in Table 9.

Acanthite fills fissures several microns thick in quartz–adularia aggregate and forms small segregations in aggregate with native silver and polybasite (Fig. 10c). Acanthite forms two generations: the first

Table 6. Results of Au, Ag, and REE sampling for Valunistoe deposit

Ord. nos.	Sample nos.	Element content, g/t																	$\sum REE_N$	Eu/Sm_N
		Ag	Au	Y	La	Ce	Pr	Nd	Sm	Eu	Gd	Tb	Dy	Ho	Er	Tm	Yb	Lu		
1.	V20a	43.15	42.78	12.72	5.58	18.07	2.88	13.01	2.77	0.499	3.32	0.415	2.29	0.409	1.10	0.117	0.57	0.070	155	0.5
2.	V-20c	10.70	10.60	13.91	11.00	39.79	6.11	26.53	4.76	0.719	4.56	0.505	2.55	0.458	1.32	0.149	0.82	0.104	274	0.4
3.	V-21	0.87	0.88	1.91	0.67	1.34	0.18	0.82	0.27	0.076	0.30	0.057	0.38	0.072	0.19	0.023	0.01	0.011	16	0.8
4.	V-22a	28.40	75.70	0.26	0.35	0.66	0.07	0.27	0.06	0.281	0.08	0.009	0.06	0.017	0.06	0.006	0.01	0.008	9	12.9
5.	V-22c	95.20	57.50	0.29	0.34	0.76	0.13	0.60	0.12	0.485	0.24	0.019	0.08	0.017	0.07	0.007	0.01	0.009	14	11.2
6.	V-23	357.88	0.97	0.77	1.73	3.56	0.44	1.88	0.33	0.130	0.37	0.040	0.19	0.036	0.11	0.012	0.03	0.010	25	1.1
7.	V-24a	127.00	16.60	9.20	11.56	27.99	4.07	17.51	3.67	1.201	4.83	0.518	2.68	0.495	1.50	0.196	1.36	0.193	240	0.9
8.	V-24c	4.78	1.65	11.86	13.92	30.27	3.64	14.72	3.02	0.567	2.85	0.523	2.37	0.470	1.26	0.194	1.26	0.220	221	0.5
9.	V-67	3.35	0.10	7.85	8.32	20.88	2.65	12.24	2.71	0.634	2.78	0.404	2.24	0.420	1.23	0.152	1.03	0.153	170	0.6
10.	V-68	1.35	0.22	9.61	11.45	29.50	4.23	20.95	4.32	0.957	4.29	0.590	2.82	0.506	1.98	0.173	1.17	0.169	249	0.6
11.	V-69	0.95	0.09	12.81	24.03	62.40	9.60	42.93	8.05	1.310	6.55	0.814	3.37	0.478	1.14	0.113	0.66	0.092	439	0.4
12.	V-70	6.26	0.06	13.85	12.85	32.50	4.80	24.04	5.17	1.346	4.90	0.669	3.42	0.596	1.67	0.204	1.36	0.201	285	0.7
13.	V-71	2.75	3.39	4.77	3.22	12.64	1.69	8.30	2.24	0.513	2.16	0.285	1.26	0.194	0.46	0.047	0.30	0.043	99	0.6
14.	V-72	4.23	0.22	10.59	3.34	8.26	0.95	4.46	1.06	0.362	1.53	0.282	1.76	0.331	1.11	0.118	0.75	0.102	84	0.9
15.	V-73	0.71	0.26	3.08	0.79	1.65	0.22	0.97	0.25	0.108	0.41	0.096	0.47	0.097	0.22	0.042	0.16	0.030	21	1.2
16.	V-74	3.43	0.80	2.27	0.77	1.63	0.20	0.93	0.22	0.429	0.30	0.100	0.30	0.070	0.15	0.115	0.55	0.907	55	5.2
17.	V-75	8.13	0.19	0.25	0.24	0.46	0.05	0.17	0.03	0.027	0.05	0.011	0.05	0.011	0.03	0.007	0.09	0.009	4	2.4
18.	V-76	1.13	0.03	0.33	0.29	0.50	0.11	0.40	0.08	0.208	0.08	0.011	0.05	0.015	0.04	0.011	0.15	0.044	10	6.9
19.	V-77	0.90	0.05	7.47	9.61	21.75	2.95	12.01	2.70	1.152	2.89	0.352	1.87	0.357	1.18	0.138	1.04	0.144	180	1.2
20.	V-78	1.06	1.07	15.63	15.54	36.42	4.71	20.54	4.29	1.479	4.17	0.592	3.13	1.180	1.65	0.245	1.71	0.307	298	0.9
21.	V-79	0.84	0.61	6.75	6.60	15.99	2.26	10.26	2.20	0.982	2.30	0.297	1.64	0.313	1.05	0.120	0.82	0.122	142	1.2
22.	V-80	0.79	0.25	14.28	14.40	36.05	5.02	20.17	4.95	1.332	4.71	0.656	3.50	0.651	2.06	0.252	1.74	0.243	295	0.7
23.	V-81	4.44	0.46	6.11	8.86	19.20	2.88	11.56	3.01	1.022	3.55	0.375	1.54	0.262	1.54	0.099	0.73	0.104	172	0.9
24.	V-82	0.80	0.11	3.19	0.38	0.73	0.07	0.28	0.06	0.251	0.11	0.019	0.07	0.018	0.05	0.012	0.16	0.053	11	10.9
25.	V-83	0.37	0.08	0.92	0.52	1.18	0.13	0.62	0.17	1.238	0.31	0.051	0.18	0.060	0.19	0.035	0.21	0.063	32	19.5
26.	V-84	0.59	0.02	3.41	9.46	20.50	2.38	9.10	1.56	0.243	1.17	0.237	0.60	0.137	0.44	0.070	0.50	0.089	125	0.4
27.	V-85	0.56	0.02	0.45	0.51	0.68	0.11	0.41	0.07	0.159	0.09	0.011	0.06	0.012	0.03	0.007	0.11	0.032	9	6.3
28.	V-86	0.56	0.03	0.64	0.44	0.92	0.11	0.45	0.11	0.332	0.13	0.019	0.10	0.022	0.06	0.014	0.21	0.061	14	8.6
29.	V-87	0.95	0.12	7.77	17.03	38.56	4.69	20.49	3.61	0.703	3.30	0.453	2.39	0.450	1.38	0.175	1.19	0.178	263	0.5
30.	V-88	7.13	0.59	0.62	0.52	1.20	0.20	1.00	0.17	0.760	0.27	0.019	0.10	0.021	0.10	0.013	0.12	0.025	22	12.5
31.	V-89	0.58	0.40	0.62	0.57	1.11	0.13	0.52	0.12	0.556	0.17	0.019	0.12	0.021	0.07	0.019	0.32	0.096	20	12.8
32.	V-90	4.10	0.40	1.53	1.39	2.94	0.35	1.44	0.31	0.090	0.29	0.050	0.27	0.057	0.17	0.024	0.18	0.035	23	0.8
33.	V-91	1.58	0.28	26.38	31.44	75.68	8.96	38.10	7.38	1.470	7.12	0.989	5.70	1.096	3.26	0.448	3.14	0.473	531	0.5

Samples V-20ac, and V-22 to V-24 are Au–Ag epithermal ores; V-80, V-78, V-87, and V-91, host rocks; V-21, V-69, V-75, V-76, and V-81, nonore quartz veins; V-67, V-68, V-70, V-71, and V-77, hydrothermal breccias; V-72 and V-84, fluorite; V-73, V-74, V-79, V-82, V-83, V-85, V-86, and V-88 to V-90, calcite and calcite-bearing veins.

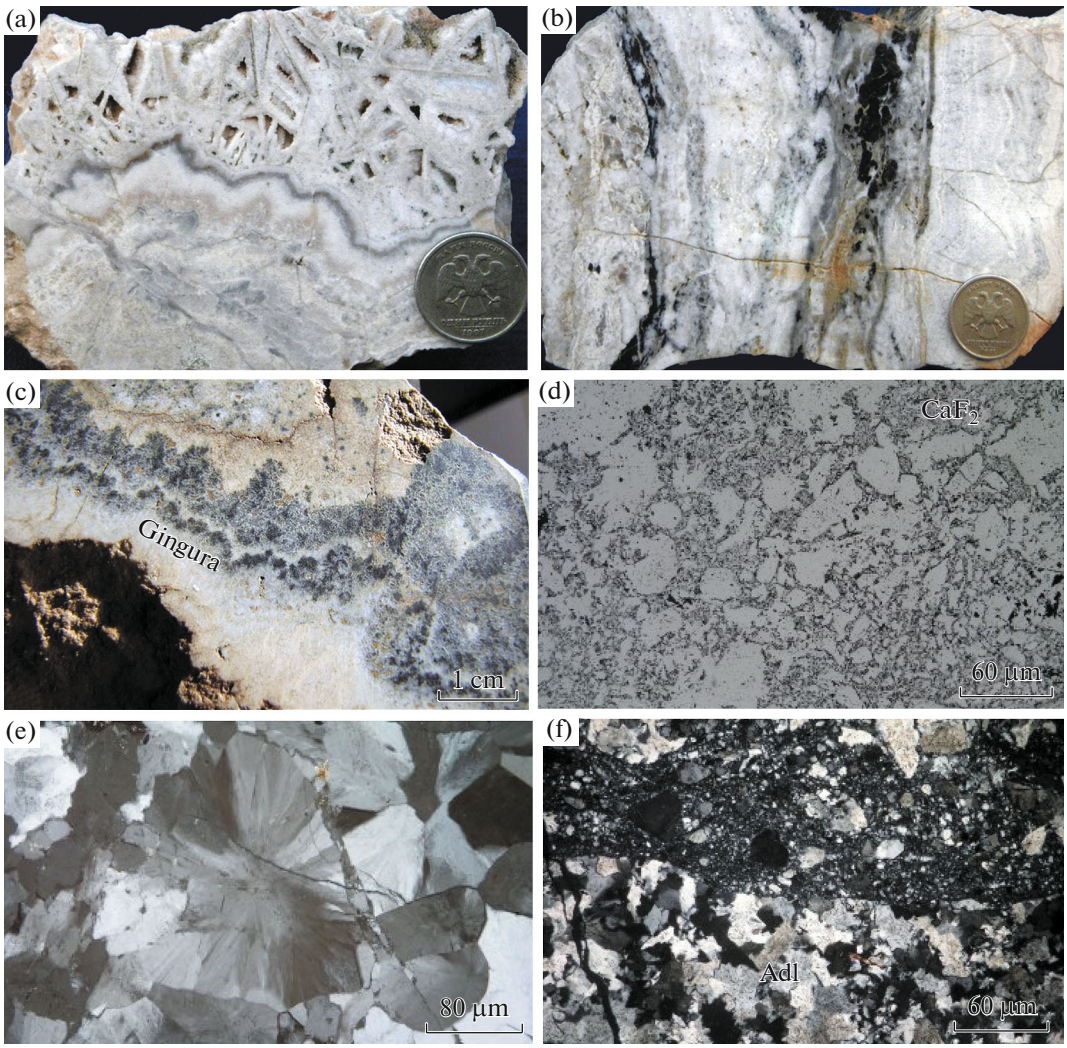

Fig. 9. Structural–textural peculiarities of Valunistoe deposit ore-bearing veins: (a) adularia–quartz vein possessing colloform and framed-platy structures, Main vein zone, trench 106 (I.S. Raevskaya's collection); (b) adularia–quartz vein rhythmically banded structure, Main vein zone, trench 106 (I.S. Raevskaya's collection); (c) gingura (scalloped texture, bands of Ag minerals and electrum in adularia–quartz vein, Main vein zone (collection of museum of Russian State Geological Survey University); (d) breccia structure (fluorite cementing fragments of pennant quartz and adularia); (e) radial-fibrous quartz; (f) microbreccia containing adularia and quartz fragments and cutting adularia band in vein.

likely precedes native minerals (and may contain Se), while the second does not contain Se, forms solid and discontinuous rims on earlier segregated Ag minerals, and also fills cracks in quartz. The composition of acanthite is presented in Table 9.

Polybasite is observed in the form of isometric, but, more frequently, elongated inclusions in acanthite and in native Ag and Au (Fig. 10c). Segregations range in size from several to 90 μm. Polybasite is replaced with native silver. The composition of polybasite is presented in Table 9.

RESULTS OF FLUID INCLUSION STUDIES

Visual examination of fluid inclusions in quartz and calcite from ores of the Valunistoe deposit allowed us, based on their filling, to identify one type of inclusions: two-phase gaseous–liquid inclusions of weakly mineralized solutions with a gas bubble making up 5–20 vol % of the total volume of each inclusion (Figs. 11a–d). For thermo- and cryometric studies, we chose, first of all, fluid inclusions located in growth zones or individual quartz grains, homogeneously distributed over the volume and which we attributed to be primary inclusions.

The results of thermo- and cryometric studies for more than 100 individual fluid inclusions in quartz and calcite from the Valunistoe deposit (Table 10, Fig. 11e) showed that Na and K chlorides were predominant in solutions of two-phase fluid inclusions, as is indicated by the eutectic points of solutions from inclusions in the temperature range from –25 to –33°C. Full homogenization of fluid inclusions takes place in quartz at temperatures from 203 to 284°C, while in

Table 7. Abundance of minerals in ores of Valunistoe deposit

Relative abundance	Hypogene ore minerals	Hypergene minerals	Non-ore minerals
Primary	Pyrite, acanthite, cahlcopyrite, galena, sphalerite		Quartz, adularia
Secondary	Native Au, native Ag, polybasite, acanthite, Se-acanthite **, minerals of Ag–Te–Se–S* system	Iron hydroxides	Calcite, fluorite, epidote, sericite, chlorite, pyrophyllite, albite
Rare	Pearceite, magnetite, hematite, marcasite, freibergite*, tetrahedrite, bournonite, minerals of Ag–Te–Se*, Ag–Se–S*, and Ag–Te–S* systems, hessite*, matildite*, minerals of Ag–Bi–Te–S* and Ag–Pb–Te–S* systems, Bi tellurides*, stromeyerite*, Ag sulfoselenide*	Covelline, chalcosine, bornite, anglesite, Pb oxides, native Cu, native Ag and Se-acanthite**, kaolinite, smectite, Ag tellurates*, Ag selenates*, malachite*	Fe-Mg carbonate, gypsum, zeolite

* Minerals reported in previous studies (Bryzgalov and Krivitskaya, 1998; Novoselov et al., 2009; Shabalin et al., 1995*).
** Native Ag and Se-acanthite were found in both hypogene and hypergene associations.

Table 8. Representative analyses of native Au (1–4) and Ag (5–9) from Valunistoe deposit, in wt %

Component	1	2	3	4	5	6	7	8	9
Au	73.60	61.41	60.39	59.11	36.95	3.21	0.89	0.28	–
Ag	19.01	40.33	38.87	40.59	54.86	89.36	94.86	89.14	91.53
Hg	7.38	–	–	–	6.18	7.87	5.55	11.84	9.35
Cu	–	0.04	0.06	0.80	–	–	0.26	0.13	0.58
Bi	–	–	–	–	–	–	0.35	0.30	–
Total	99.99	101.78	99.32	100.50	97.99	100.44	101.91	101.69	101.46
Fineness	736	603	608	588	377	32	9	3	0

Table 9. Compositions of ore minerals from Valunistoe deposit, based on micro-X-ray spectral analysis (wt %)

Components	1	3	4	5
Ag	88.10	76.50	76.66	73.88
S	12.43	1.14	1.06	13.91
Se	–	23.20	23.17	2.26
Cu	–	1.00	0.81	2.22
Hg	–	0.03	0.19	–
As	–	–	–	1.20
Sb	–	–	–	7.15
Sum	100.89	101.86	101.89	100.62
Coefficients in crystallochemical formulas				
Ag	2.03	2.02	2.03	15.80
S	0.97	0.10	0.09	10.01
Se	–	0.84	0.84	0.66
Cu	–	0.04	0.04	0.81
Hg	–	–	–	–
As	–	–	–	0.37
Sb	–	–	–	1.35
Mineral	Acanthite Ag_2S	Naumannite Ag_2Se	Naumannite Ag_2Se	Polybasite $(Ag,Cu)_{16}Sb_2S_{11}$

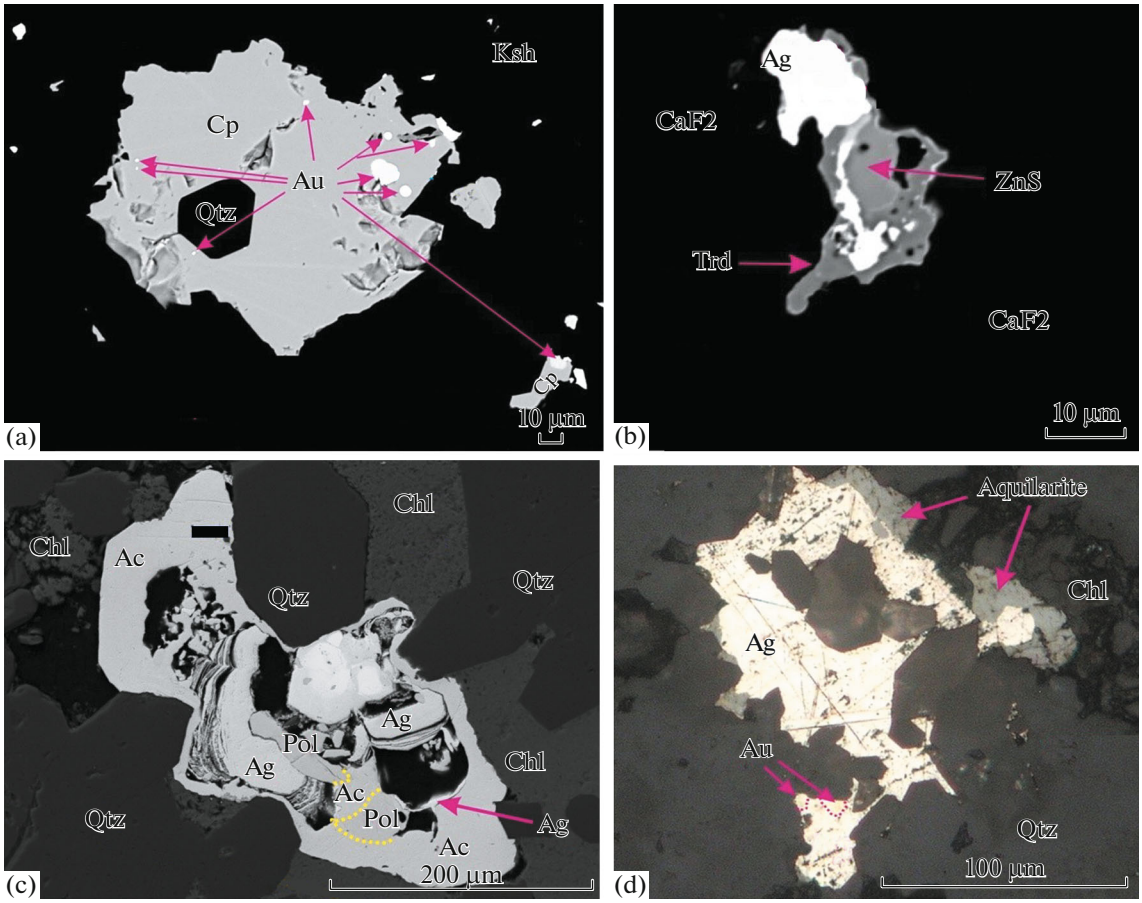

Fig. 10. Main ore minerals of Valunistoe deposit. Images (a–c) are in back scattered electrons and (d) is a micrograph. (a) Multiple fine native Au segregations in chalcopyrite (Cp) in adularia matrix; (b) native Ag segregate at contact between intergrowth of tetrahedrite (Trd) and sphalerite in fluorite matrix; (c) aggregate of polybasite (Pol) and native Ag in acanthite (Ac) matrix; (d) native Ag in aguilarite. Qtz—quartz; Ksh—adularia; Chl—chlorite.

calcite, at temperatures from 174 to 237°C, with the salt concentration varying from 0.2 to 0.7 wt % NaCl equiv for inclusions in quartz and calcite (Table 10). Fluid density changes from 0.90 to 0.73 g/cm^3. Notably, fluids of the Valunistoe and Kupol deposits have very close physicochemical parameters (Volkov et al., 2012).

The bulk chemical composition of fluids from inclusions in quartz collected at the Valunistoe deposit is shown in the chart (Fig. 11f). Among cations, K and Na play the key role in the fluid (2.26 and 0.94 g/kg of H_2O, respectively), while Mg is subordinate in amount (0.04). Significant amounts of such components as HCO_3^-, CO_2, and CH_4 (3.11, 5.4, and 0.07 g/kg of H_2O, respectively) are found. Additionally, the following trace elements were revealed in the fluid composition (mg/kg of H_2O): As (128), Li (18.0), B (41.8), Rb (1.1), Cs (0.24), Sr (4.1), Sb (22.0), Cu (3.2), Zn (26.7), Cd (0.02), Pb (2.1), Bi (0.09), Th (0.01), Ga (0.05), Ge (0.18), Mn (13.1), Fe (104), Co (1.35), V (0.09), Y (0.01), Zr (0.36), Sn (0.07), Ba (1.4), W (0.003), Tl (0.03), and REE (0.05). The main parameters of the fluid are as follows: CO_2/CH_4 = 76.57, Na/K = 0.41, and K/Rb = 238.9.

In fluid composition, the Valunistoe deposit is similar to the adjacent Zhil'noe (Elmanov et al., 2018). In addition, the composition of Valunistoe deposit fluids is similar, in some degree, to fluids from the Kupol and Dvoinoe deposits (Volkov et al., 2012). However, the Kupol deposit differs in a relatively higher mineralization of fluids.

Low salt concentrations and ore formation temperatures are analogous to the fluids of epithermal low-sulfidized deposits (see (Simmons et al., 2005, Bodnar et al., 2014) and others). Given the extremely low mineralization of fluid inclusions in quartz, solutions that formed quartz veins were most likely represented by condensed vapor that separated from the hydrothermal fluid as a result of boiling during an abrupt change in pressure.

DISCUSSION

An important structural feature of the Valunistoe deposit (formation of Au–Ag-bearing vein zones) is

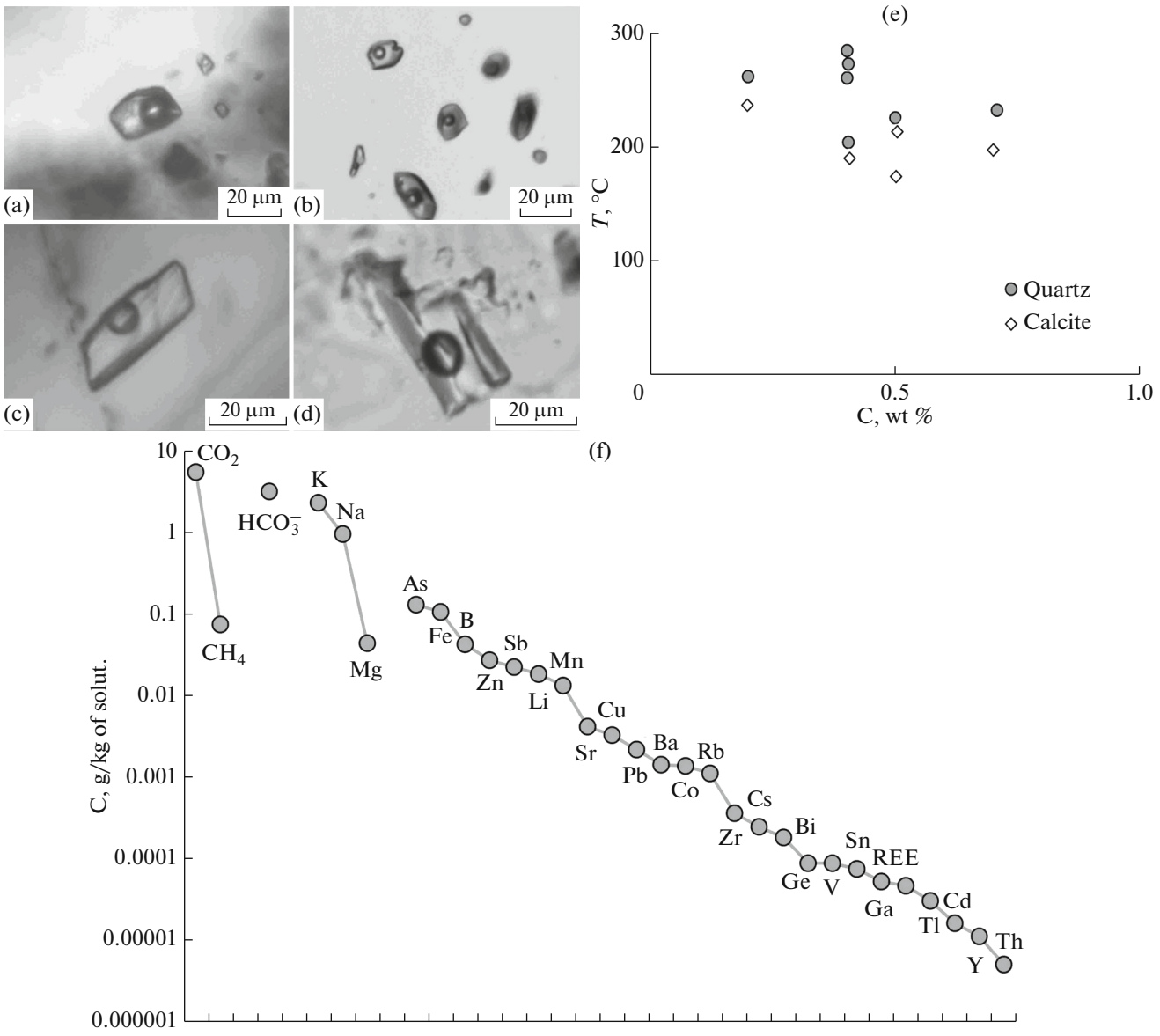

Fig. 11. Images of fluid inclusions in quartz (a, b) and calcite (c, d) at Valunistoe deposit; (e) temperature versus salt concentration diagram for Valunistoe deposit; (f) composition of mineral-forming fluids of Valunistoe deposit.

controlled by subvolcanic bodies of fluidal rhyodacites (Fig. 3). Another structural feature of the deposit, important for the industrial aspect, is the significant extent of ore-bearing zones along strike (more than 1.5 km). These features are likely caused by the formation of ore zones at the deposit in vent facies of a paleovolcanic edifice. This explanation is supported (a) by the presence of a large amount of breccias and megabreccias, characterized by cascading overgrowth structures of chalcedony–adularia aggregate (with Au–Ag mineralization) after fragments with various petrographic composition, in orebodies of the deposit, and (b) by the diversity of breccias marking ore zones (Figs. 4b, 4c). Note that the large Kupol and Dvoinoe deposits in the Chukotka segment of the OChVB are characterized by similar structural–geological features (Volkov et al., 2012, 2018).

Based on structural–textural analysis, the general sequence of vein minerals can be represented as follows: (1) fine-grained and cryptocrystalline nonore quartz that is often included in cement of explosive breccias (Fig. 4b); (2) early fine- and medium-grained quartz and adularia with impregnations of ore minerals; (3) coarse-grained radial-fibrous, pennant, and combed quartz (Fig. 9e) with multiple dark-colored microinclusions arranged zonally or sometimes sectorially; (4) fine-grained to fine-crystalline adularia observed in banded veins, usually having rhombic or xenomorphic crystals (Fig. 9f); (5) fluorite forming crosscutting veinlets or filling caverns in aggregates of

coarse-grained quartz (Fig. 9d); (6) intravein fragmentation and development of veinlets and veins of coarse-grained and platy calcite and thin veinlets of nonore fine-grained quartz; (7) later fibrous gypsum (selenite). The sequence of mineral formation is shown in Fig. 12.

In adularia–quartz veins enriched in Au and Ag, deposition started from fine-grained quartz and fine-grained adularia, with the primary concentration of microgranular ore mineralization in this aggregate. Weak crystallization of these aggregates suggests that their deposition rate was most likely high and this probably predetermined the preferred localization of the certain part of Au and Ag minerals along the endomorphic contact parts of veins. Deposition of ore minerals began from sulfides (pyrite, chalcopyrite, galena, and sphalerite), then acanthite, polybasite, and native gold, which formed interpositions in sulfides. In this sequence, native gold is most likely the latest, because it is often localized in fissures within chalcopyrite, at contacts between sulfides (pyrite and chalcopyrite) and acanthite.

Then, depending on the degree of opening of cavities and fissures, growth of quartz and adularia took place; in places, their zonal segregation occurred to form individual interbeds (bands). Insignificant recrystallization and coarsening of ore minerals are possible, at that. In particular, Au–Ag mineralization is sometimes reported in coarse-grained adularia and in crystal interstices with respect to coarse-grained pennant quartz. Probably, it is this time when Se-varieties of Ag minerals appeared.

At the postmineral stage, calcite veins and veinlets formed at the deposit (Fig. 5). Calcite normally does not contain ore minerals, while rarely observed sphalerite and native gold are most likely relict, not redeposited units. Sometimes calcite is crosscut by relatively short curved veinlets of weakly crystallized quartz containing fine pyrite and chlorite.

Hypergene alterations of ores are relatively weakly manifested, although their traces (in the forms of goethite, covellite, bornite, native copper, anglesite or Pb oxide, and clay minerals) occur in samples collected both at the surface and at depth (in wells). Acanthite and native silver sometimes develop after Ag minerals. The earlier studies also noted a high fineness of native gold of hypergene origin (Shabalin et al., 1995*).

Our study of the spatiotemporal and physicochemical conditions of calcite formation allowed us to point out its important role in the formation of orebodies at the Valunistoe deposit. Its extensive distribution of calcite in ore veins is a specific feature compared to the other epithermal deposits in the Chukotka segment of the OChVB. In particular, carbonate minerals are virtually absent at the Kupol and Dvoinoe deposits (Volkov et al., 2012, 2018). Both geological fund publications on the Valunistoe deposit and subsequent studies (Volkov et al., 2006; Struzhkov, 2010) mention only the presence of calcite in quartz veins, without any data on the extent and features of its development, as well as on the postmineral (along with gypsum and fluorite) formation of this mineral.

We have established a very broad distribution of coarse-grained and platy calcite both in calcite veins and in quartz–adularia and quartz–fluorite veins of orebodies at the Valunistoe deposit. We have also revealed the main features of its formation, one of which is the ability of calcite to partially or almost completely fill the vein space previously filled with quartz–adularia aggregate of varying morphology; in fact, its capability of replace (dilute) this aggregate remained in the form of relic fragments of uneven-sizes. Judging by the data obtained when studying the core recovered from the VD-12-1301 well, the amount of calcite in adularia–quartz veins clearly increases with depth. Ore mineralization is rarely found in calcite proper.

Note that calcite deposition was quite often preceded by the formation of predominantly colorless fluorites that cut through, cemented, and leached brecciated quartz–adularia veins, probably indicating the active participation of F-bearing fluids in the destruction and subsequent replacement of quartz veins with calcite. Such a suggestion agrees with the ability (well known in inorganic chemistry) of high-HF solutions to transform quartz into a volatile compound (SiF_4) at temperatures of about 150–200°C, and also with the fact that carbon dioxide solutions are weakly aggressive to quartz in these conditions (Remy, 1960).

Thus, formation of Au–Ag mineralization of the Valunistoe deposit demonstrates two independent, uneven-aged stages. These stages essentially differ in the character of vein mineralization and metasomatic alterations of rocks in the near-vein space, in mineral compositions and geochemical properties of ores.

At the first stage typical quartz–adularia veins and veinlets of various morphologies, with a broad distribution of breccias (including explosive ones), were formed. Their formation was accompanied by chlorite-epidote alterations in rocks, being consistent with quite high temperature of their formation (up to 350°C, based on the studies of fluid inclusions in quartz).

The composition of propylite-hosted epidote can be an indicator of depth level of mineral-forming processes (Rusinov, 1989). Judging by the composition of epidote from core samples (Table 1), propylitization conditions at the Valunistoe deposit correspond to medium to low depth levels (Rusinov, 1989).

The first stage terminated with deposition of predominantly streaky ore mineralization in association with fine-grained quartz. This mineralization is represented by acanthite and native gold (Ag > 50%), as well as by Ag-bearing sulfosalts and Zn, Pb, and Cu sulfides with the predominance of Zn and Pb). Ores are characteristic of high values indicatory Au/Ag ratio

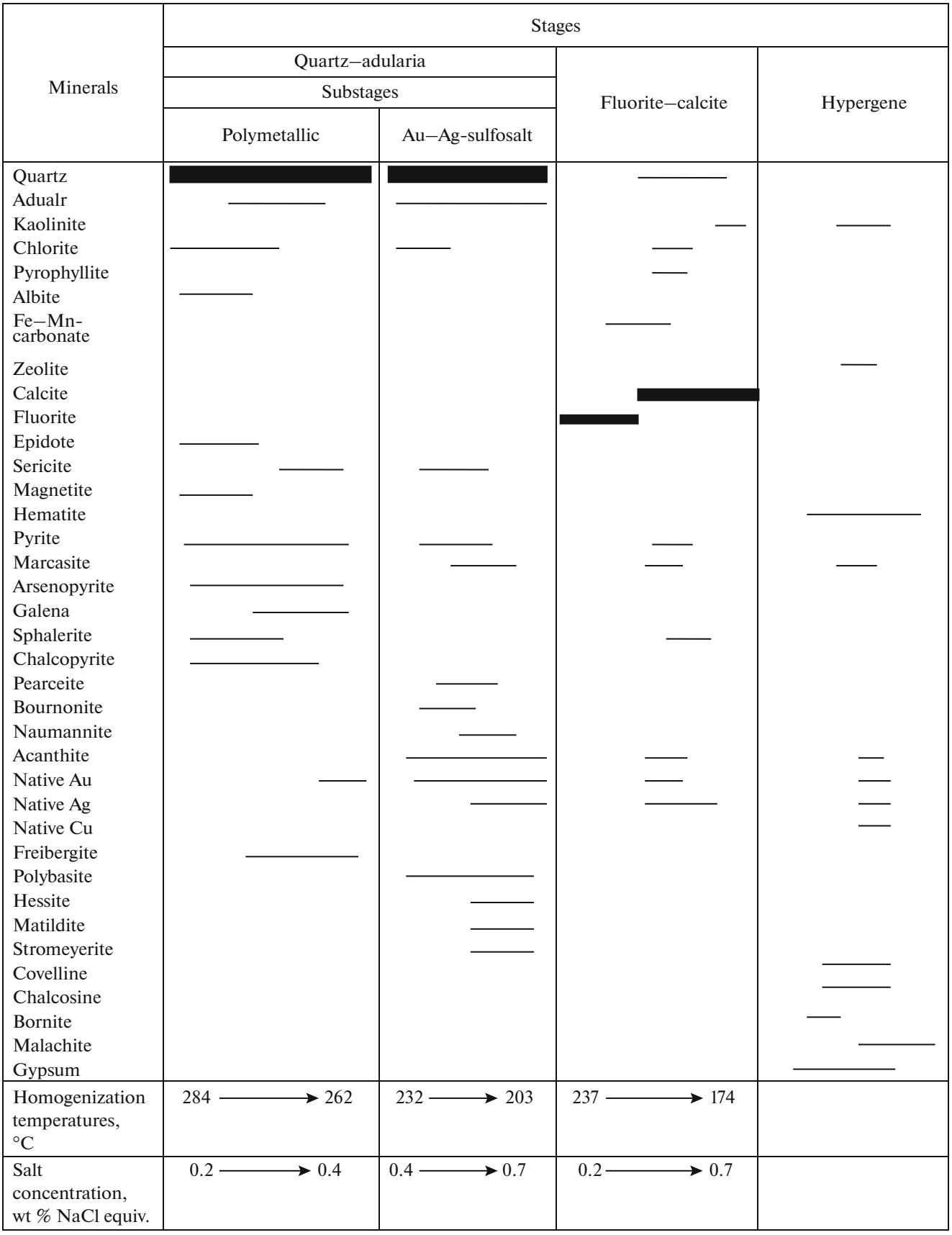

Fig. 12. Sequence of mineral formation.

(1 : 50 to 1 : 70, and up to 1 : 100), i.e., showing the clear predominance of Ag in them.

The second stage of mineralization is distinguished mainly by the broad development of calcite and, at a significantly smaller degree, fluorite in quartz–adularia veins. Note that intravein fragmentation was followed by partial (up to almost complete) replacement or primary quartz–adularia aggregate with calcite, and also deposition of finely impregnated ore mineralization in association with colloform and combed quartz and brownish green ferruginous chlorite (Table 2).

In the near-vein space, along with propylitization, other, more low-temperature metasomatic rock alteration processes took place, in particular, K-feldspathization, sericitization, and argillization. They correspond to lower temperature of calcite formation (up to 240°C) inferred from microthermometry data on fluid inclusions.

Second stage Au–Ag mineralization is represented by native gold, with a considerably lower amount of acanthite and Ag-bearing sulfosalts, and also by native silver, Sb- and Se-bearing sulfosalts, and Hg-bearing native gold and silver. Contrary to the first mineral association, it is characteristic of low values of indicatory Au/Ag ratio (less than 1 : 10), i.e., showing the predominance of Au in ores, as well as appearance of bonanzas with high Au contents (more than 70 g/t).

We should also note another specific feature of the Valunistoe deposit: with intensive intravein development of calcite, Au–Ag mineralization appears as though it has extruded into the near-vein space consisting of brecciated metasomatically altered rocks with a dense network of quartz–adularia and other veinlets. Notably, samples from large calcite veins contain insignificant amounts of Au (up to 0.59 g/t, sample V-88), evidently owing to rare relict quartz–adularia composition. In turn, this indicates redeposition of ore components with their possible spatial separation and formation (in favorable settings) of rich bonanza ores with predominant Au.

The appearance of fluorite at the late stages is related to F sublimation from Sn-bearing intrusions during postintrusive volcanic activity, while the formation of Sb minerals and Hg-bearing native gold and silver can be caused by the metallogenic specialization of the area. Fluorite cement of early mineral parageneses indicates that this mineral marks postmineral tectonics and induces metamorphic effect on Ag minerals and redistribution of ore material.

Thus, the Au–Ag ores of the Valunistoe deposits formed as a result of spatially combined hydrothermal processes, which were, however, significantly differentiated in time and likely related to noncoeval stages of volcanic activity in the OChVB (Akinin, 2011). This conclusion is of both theoretical and essentially practical value for appraising productivity of veins.

It is known that trace elements and REE react to oxidizing–reducing conditions of natural environments, enabling them to be used as geochemical indicators of sources of material and assessing the formation conditions of volcanogenic mineralization.

The U/Th ratio in the rich ores of the Valunistoe deposits (Tables 4, 5) is considerably greater than 0.75, varying from 1.12 to 4.26, which indicates reducing formation conditions (Jones and Manning, 1994).

The Co/Ni ratio in ores (Table 6) ranges from 0.066 to 0.22, which is characteristic of mixing of medium- and low-temperature meteoric hydrothermal fluids and high-temperature magmatic fluid (Kun et al., 2014).

In addition, the ores are evidently enriched in LREE and depleted in HREE and have Hf/Sm, Nb/La, and Th/La ratios less than 1 (Table 6). Hence, the ore-forming fluids belonged to a $NaCl–H_2O$ hydrothermal system enriched in Cl with respect to F (Oreskes and Einaudi, 1990), which corresponds to the results of fluid inclusion studies in ore quartz (see above).

The Y/Ho ratio in ores varies from 25.27 to 33.59 (Table 6), which corresponds to the interval reported in modern hydrothermal fluids from back-arc basins (Bau, 1991; Jones and Manning, 1994; Monecke et al., 2002).

The Valunistoe deposits demonstrated quite low ∑REE values (from 2.88 to 20.07 g/t) (Tables 6, 7). Epithermal ores of many deposits are characterized by similar values, e.g., the Qurama Range in Uzbekistan, the area of Banska-Stiavnica in Slovakia (Vinokurov et al., 1999), and deposits of the Russian Northeast (Dvoinoe, Kubaka, Birkachan, etc.) (Volkov et al., 2017).

Eu and Ce anomalies are usually considered as markers of oxidizing-reducing potential of the ore formation environment (Bortnikov et al., 2007; Goryachev et al., 2008). In samples from ores of the Valunistoe deposit, Eu/Eu* values are positive (>1), while Ce/Ce* are negative ones (close to 1), at $\sum REE_N > 20$ (Table 7); the only exclusion is rich samples (V-1, V-22) where the pattern is opposite at $\sum REE_N < 5$. The former combination of Eu/Eu* and Ce/Ce* indicates oxidizing conditions during ore deposition, while the latter (characteristic of rich ores) corresponds to reductive conditions. It is obvious that $\sum REE_N$ values and the character of lanthanides distribution on veins of predominantly breccias structure directly depends on the presence and amount of the host rock fragments, because quartz veins proper differ in very low REE concentrations. Hence, we can suggest that the host rocks might have been the source of REE and other trace elements for ore-forming fluids that produced this deposit.

It should be noted that increased REE contents in quartz and carbonate veinlets can be related to REE presence in fluid inclusions and/ore in the form of of microinclusions of such REE minerals as monazite and xenotime (Novgorodova et al., 1984; Vinokurov et al., 1999).

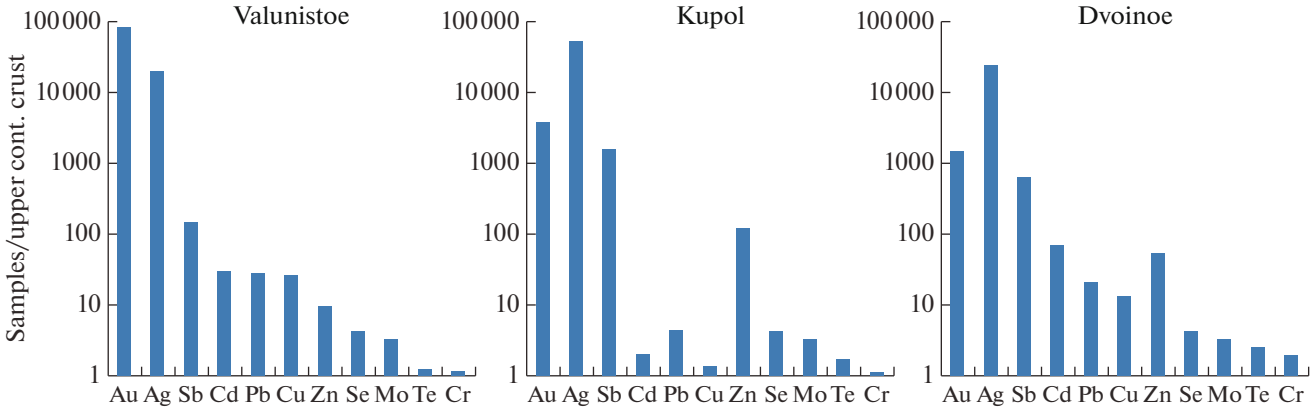

Fig. 13. Distribution of main trace elements in epithermal Au–Ag ores of Valunistoe, Kupol, and Dvoinoe deposits, normalized to average values for upper crust (Taylor and McLennan, 1985).

The presence of positive Eu anomalies in veins of different compositions suggests a deep source of solutions, at least corresponding to the lower crust (Vinokurov, 1996), and is also considered an indicator of the high productivity of ores from epithermal deposits (Vinokurov et al., 1999; Volkov et al., 2018).

Comparative analysis of the averaged geochemical spectra of the typical ores from three large Au–Ag deposits of the OChVB (Valunistoe, Kupol, and Dvoinoe) showed significant differences from each other in both trace elements and enrichment factors (Fig. 13), indicating the different geochemical specialization of the areas of these deposits. The Valunistoe deposit differs from the Kupol and Dvoinoe in the absence of As in ores, the presence of Se, and higher contents of such chalcophile elements as Ag, Cu, Pb, Zn, and Cd (Fig. 13).

CONCLUSIONS

The data provided in the present study are of practical value for regional forecasting–metallogenic maps, explorations, and appraisals of epithermal Au–Ag deposits.

The results give grounds to reliably attribute the Valunistoe deposit to the low-sulfidized epithermal class and to expect that its productive epithermal veins reach down to 400 m depth or more. A similar mineralization range has been established at the Kupol deposit, which is analogous to the Valunistoe in geological structure and where ore-bearing veins reach depths of more than 450 m (Volkov et al., 2012).

The mineralogical–geochemical and thermobarogeochemical features of the ores indicate the mixing of ore-bearing fluids with highly aerated meteoric waters, a low level of erosional truncation, and a relationship with the copper–porphyry ore-forming system. In turn, the large extent of the ore-forming system allows us to expect the discovery of new rich orebodies (including those not reaching the surface) within the Valunistoe ore field.

FUNDING

The study was supported by the Russian Foundation for Basic Research (project no. 18-05-70001).

CONFLICT OF INTEREST

The authors declare that they have no conflict of interest.

REFERENCES

Akinin, V.V. and Miller, E.L., Evolution of calc-alkaline magmas of the Okhotsk–Chukotka volcanic belt, *Petrology,* 2011, vol. 19, no. 3, pp. 249–290.

Bau, M., Rare–earth element mobility during hydrothermal and metamorphic fluid–rock interaction and the significance of the oxidation state of europium, *Chem. Geol.,* 1991, vol. 93, pp. 219–230.

Belyi, V.F., *Geologiya Okhotsko–Chukotskogo vulkanogennogo poyasa* (Geology of the Okhotsk–Chukotka Voclanogenic Belt), Magadan: SVKNII DVO RAN, 1994.

Bodnar, R.J. and Vityk, M.O., Interpretation of microthermometric data for H_2O–NaCl fluid inclusions, *Fluid Inclusions in Minerals: Methods and Applications,* Siena: Pontignano, 1994, pp. 117–130.

Bodnar, R.J., Lecumberri–Sanchez, P., Moncada, D., and Steele–MacInnes, P., *Fluid inclusions in hydrothermal ore deposits, Reference Module in Earth Systems and Environmental Sciences, Treatise on Geochemistry,* 2nd Ed. (Elsevier, 2014), 119–142.

Borisenko, A.S., Cryometric study of salt composition of gas–liquid inclusions in minerals, *Geol. Geofiz.,* 1977, no. 8, pp. 16–27.

Bortnikov, N.S., Geochemistry and origin of the ore-forming fluids in hydrothermal–magmatic systems in tectonically active zones, *Geol. Ore Deposits,* 2006, vol. 48, no. 1, pp. 1–22.

Bortnikov, N.S., Gamyanin, G.N., Vikent'eva, O.V., Prokof'ev, V.Yu., Alpatov, V.A., and Bakharev, A.G., Fluid composition and origin in the hydrothermal system of the Nezhdaninsky gold deposit, Sakha (Yakutia), Russia, *Geol. Ore Deposits,* 2007, vol. 49, no. 2. pp. 87–128.

Brown, P., Flincor: a computer program for the reduction and investigation of fluid inclusion data, *Am. Mineral.,* 1989, vol. 74, pp. 1390–1393.

Bryzgalov, I.A. and Krivitskaya, N.N., *Composition of silver minerals of the Ag–Pb–Bi–Te–S system of the Valunistoe deposit, Northeast Russia, Rol' mineralogii v razvitii mineral'no–syr'evoi bazy blagorodnykh metallov i almazov XXI veka (Role of Mineralogy in the Development of the Raw-Mineral Base of Noble Metals and Diamonds of 21th Century)*, Moscow: IGEM RAN, 1998, pp. 28–30.

Sidorov, A.A., Belyi, V.F., Volkov, A.V., Alekseev, V.Yu., and Kolova, E.E., The gold–silver Okhotsk–Chukotka volcanic belt, *Geol. Ore Deposits,* 2009, vol. 51, no. 6, pp. 441–455.

Elmanov, A.A., Prokof'ev, V.Yu., Volkov, A.V., Sidorov, A.A., and Voskresenskii, K.I., First data on formation conditions of the Zhilnoye Au–Ag epithermal gold deposit (Eastern Chukotka, Russia), *Dokl. Earth Sci.,* 2018, vol. 480, no. 6, pp. 725–729.

Goryachev, N.A., Vikent'eva, O.V., Bortnikov, N.S., Prokof'ev, V.Yu., Alpatov, V.A., and Golub, V.V., The world-class Natalka gold deposit, northeast Russia: REE patterns, fluid inclusions, stable oxygen isotopes, and formation conditions of ore, *Geol. Ore Deposits,* 2008, vol. 50, no. 5, pp. 362–390.

Keithe, T., White, D., and Beeson, M., Hydrothermal alteration and self sealing in Y–7 and Y–8 drillholes in the northern part of Upper Geyser Basin, *US Geol. Soc. Prof. Paper,* 1978, vol. 1054A, pp. 34–49.

Kryazhev, S.G., Prokof'ev, V.Yu., and Vasyuta, Yu.V., Application of ICP–MS method in analyzing the composition of ore-forming fluids, *Vestn. Mosk. Gos. Univ., Ser. 4. Geol.,* 2006, no. 4, pp. 30–36.

Kun, L., Ruidong, Y., Wenyong, Ch., et al., Trace element and REE geochemistry of the Zhewang gold deposit, southeastern Guizhou province, China, *Chin. J. Geochem.,* 2014, vol. 33, pp. 109–118.

Leier, P.V., Ivanov, V.V., Ratkin, V.V., and Bundtsen, T.K., Epithermal gold–silver deposits of Northeast Russia: the first $^{40}Ar–^{39}Ar$ age determinations of the ores, *Dokl. Earth Sci.,* 1997, vol. 356, no. 5, pp. 1141–1144.

Manning, D.A.C., Comparison of geochemical indices used for the interpretation of palaeoredox conditions in ancient mudstones, *Chem. Geol.,* 1994, vol. 111, pp. 111–129.

Mineev, D.A., *Lantanoidy v rudakh redkozemel'nykh i kompleksnykh mestorozhdenii* (Lanthanides in Rare-Earth Ores and Complex Deposits), Moscow: Nauka, 1974.

Monecke, T., Kempe, U., and Gotze, J., Genetic significance of the trace element content in metamorphic and hydrothermal quartz: a reconnaissance study, *Earth Planet. Sci. Lett.,* 2002, vol. 202, nos. 3–4, pp. 709–724.

Newberry, R.J., Layer, P.U., Ganz, P.B., et al., Preliminary analysis of chronology of Mesozoic magmatism and mineralization at Northeast Russia with allowance for 40Ar/39Ar dates and trace element data of igneous and mineralized rocks, *Zolotoe orudenenie i granitoidnyi magmatizm Severnoi Patsifiki* (Gold Mineralization and Granitoid Magmatism of Northern Pacific), Magadan: *SVKNII DVO RAN*, 2000, vol. 1, pp. 181–205.

Naboko, S.I. and Glavatskikh, S.F., *Hydrothermal minerals of Goryachii Beach, Mineralogiya gidrotermal'nykh sistem Kamchatki* (Mineralogy of Hydrothermal Systems of Kamchatka), Moscow: Nauka. 1970.

Novgorodova, M.I., Veretennikov, V.M., Boyarskaya, R.V., et al., Geochemistry of trace elements in quartz, *Geokhimiya,* 1984, no. 3, pp. 370–383.

Novoselov, K.A., Kotlyarov, V.A., Belogub, E.V., Silver sulfoarsenides from ores of the Valunistoe gold–silver deposit, Chukotka, *Zap. Ross. Mineral. O-va,* 2009, vol. 138, no. 6, pp. 56–61.

Oreskes, N. and Einaudi, M.T., Origin of rare–earth element enriched hematite breccias at the Olympic Dam Cu–U–Au–Ag deposit, Roxby Downs, South Australia, *Econ. Geol.,* 1990, vol. 85, no. 1, pp. 1–28.

Polin, V.F., *Petrologiya kontrastnoi serii Amguemo–Kanchalanskogo vulkanicheskogo polya Chukotki* (Petrology of the Bimodal Series of the Amguem–Kanchalansk Volcanic Belt), Vladivostok: DVO AN SSSR, 1990.

Remy, H., *Treatise on Inorganic Chemistry* (Elsevier, London, 1956), Vol. 1.

Rusinov, V.L., *Metasomaticheskie protsessy v vulkanicheskikh tolshchakh* (Metasomatic Processes in Volcanic Sequences), Moscow: Nauka, 1989.

Sakhno, V.G., Polin, V.F., Akinin, V.V., Sergeev, S.A., Alenicheva, A.A., Tikhomirov, P.L., and Moll–Stolkap, E. J., The diachronous formation of the Enmyvaam and Amguema–Kanchalan volcanic fields in the Okhotsk–Chukotka Volcanic Belt (NE Russia): evidence from isotopic data, *Dokl. Earth Sci.,* 2010, vol. 434, no. 2, pp. 1172–1178.

Sidorov, A.A., *Zoloto–serebryanaya formatsiya Vostochno–Aziatskikh vulkanogennykh poyasov* (Gold–Silver Formation of the East Asian Volcanogenic Belts), Magadan, 1978.

Simmons, F.A., White, N.C., and John, D.A., Geological characteristics of epithermal precious and base metal deposits, *Econ. Geol.,* 2005, Vol. 100, pp. 485–522.

Struzhkov, S.F., *Province of the Okhotsk–Chukotka volcanogenic belt, Zolotorudnye mestorozhdeniya Rossii (Gold Deposits of Russia)*, Moscow: Akvarel', 2010, pp. 213–242.

Taylor, S.R. and McLennan, S.M., *The Continental Crust: its Composition and Evolution,* Oxford: Blackwell, 1985.

Vinokurov, S.F., Europium anomalies in ore deposits and their geochemical significance, *Dokl. Earth Sci.,* 1996, vol. 346, no. 6, pp. 281–283.

Vinokurov, S.F., Kovalenker, V.A., Safonov, Yu.G., and Kerzin, A.L., REE in quartz from epithermal gold deposits: distribution and genetic implications, *Geochem. Int.,* 1999, vol. 37, no. 2, pp. 145–152.

Volkov, A.V., Goncharov, V.I., and Sidorov, A.A., *Mestorozhdeniya zolota i serebra Chukotki* (Gold and Silver Deposits of Chukotka), Magadan: SVKNII DVO RAN, 2006.

Volkov, A. V., Prokof'ev, V. Yu., Savva, N. E., Sidorov, A.A., Byankin, M.A., Uyutnov, K.V., and Kolova, E.E., Ore formation at the Kupol epithermal gold–silver deposit in northeastern Russia deduced from fluid inclusion study, *Geol. Ore Deposits,* 2012, vol. 54, no. 4, pp. 295–303.

Volkov, A.V., Sidorov, A.A., Savva, N.E., Kolova, E.E., Chizhova, I.A., and Murashov, K.Yu., The geochemistry of volcanogenic mineralization in the northwestern segment of the Pacific ore belt: Northeast Russia, *J. Volcanol. Seismol.,* 2017, vol. 11, no. 6, pp. 389–406.

Volkov A.V., Sidorov A.A., Prokof'ev V.Yu., Savva N.E., Kolova E.E., and Murashov K.Yu. Epithermal mineralization in the Okhotsk–Chukchi Volcano-Plutonic Belt, *J. Volcanol. Seismol.,* 2018, vol. 12, no. 6, pp. 359–378.

Zharikov V.A., Gorbachev N.S., Lightfoot, P., and Doherty, W., Rare earth element and yttrium distribution between fluid and basaltic melt at pressures of 1–12 kbar: evidence from experimental data, *Dokl. Earth Sci.,* 1999, vol. 366, no. 2, pp. 543–545.

Translated by N. Astafiev